DOE/NASA/0167-5
NASA CR-168104
GARRETT NO. 31-3725(5)

ADVANCED GAS TURBINE (AGT) POWERTRAIN SYSTEM DEVELOPMENT FOR AUTOMOTIVE APPLICATIONS

FIFTH SEMIANNUAL PROGRESS REPORT
(JANUARY 1982 — JUNE 1982)

Engineering Staff of
Garrett Turbine Engine Company
A Division of The Garrett Corporation

December 1982

Prepared for

NATIONAL AERONAUTICS AND SPACE ADMINISTRATION
Lewis Research Center
Cleveland, Ohio 44135
Under Contract DEN3-167

for

U.S. DEPARTMENT OF ENERGY
Office of Vehicle and Engine Research and Development
Technology Development and Analysis Division
Washington D.C. 20585

DOE/NASA/0167-5
NASA CR-168104
GARRETT NO. 31-3725(5)

ADVANCED GAS TURBINE (AGT) POWERTRAIN SYSTEM DEVELOPMENT FOR AUTOMOTIVE APPLICATIONS

FIFTH SEMIANNUAL PROGRESS REPORT
(JANUARY 1982 — JUNE 1982)

Engineering Staff of
Garrett Turbine Engine Company
A Division of The Garrett Corporation

December 1982

Prepared for
NATIONAL AERONAUTICS AND SPACE ADMINISTRATION
Lewis Research Center
Cleveland, Ohio 44135
Under Contract DEN3-167

for
U.S. DEPARTMENT OF ENERGY
Office of Vehicle and Engine Research and Development
Technology Development and Analysis Division
Washington D.C. 20585

TABLE OF CONTENTS

TABLE OF CONTENTS (Cont)

LIST OF ILLUSTRATIONS

LIST OF ILLUSTRATIONS (Cont)

LIST OF ILLUSTRATIONS (Cont)

LIST OF TABLES

1.0 SUMMARY

This report describes progress and work performed by the Garrett/Ford team to develop an Advanced Gas Turbine (AGT) powertrain system for automotive applications, during the period January through June 1982. This work was performed for the Department of Energy under NASA Contract DEN3-167. This is the fifth in a series of semiannual reports. Work performed during the first four periods (References 1 through 4) initiated design and analysis, ceramic development and component testing.

Project effort conducted under this contract is part of the DOE* Gas Turbine Highway Vehicle System Program. This program is oriented at providing the United States automotive industry the high-risk long-range technology necessary to produce gas turbine powertrains for automobiles with reduced fuel consumption and reduced environmental impact. It is intended that technology resulting from this program reach the marketplace by the early 1990's.

The advanced automotive gas turbine, when installed in a Ford vehicle (3000 pounds inertia weight), will provide:

- A CFDC fuel economy of 42.8 miles per gallon based on Environmental Protection Agency (EPA) test procedures and Diesel No. 2 fuel. The AGT-powered vehicle will substantially give the same overall vehicle driveability and performance as a comparable production vehicle powered by a conventional spark-ignition powertrain system
- Emissions less than federal standards
- Ability to use a variety of fuels

The Garrett/Ford project efforts were modified during March 1981 to accommodate imposed budget constraints. The primary changes involved reducing first generation component tests, deferral of gearbox and transmission systems development, and stopping vehicular integration activities. These changes permitted concentration of remaining resources toward continued development of higher technology components and ceramics necessary for the AGT engine.

*A list of abbreviations and acronyms is presented in Appendix D, herein.

1.1 Engine/Powertrain Development

Testing was continued on S/N 001, Build 4 engine including a demonstration run for the House Science and Technology Committee visitors. The ECU was integrated and fuel system modifications were incorporated for improved atomization and lightoff characteristics. The turbine shroud support system was modified to correct a thermal misalignment problem. Thirty start/stop cycles of hot testing verified the modification and testing was resumed.

Engine power was measured at 75,000 rpm and output horsepower was 8 bhp (uncorrected) with a 1600°F turbine inlet temperature (TIT) and variable inlet guide vane (VIGV) positions of 40 to 50 degrees. This was recorded as the best attainable output power with current regenerator seal leakage. Engine idle fuel flow was measured at 2.6 lbs/hr. This is the lowest known gas turbine fuel flow recorded and is already comparable to a spark ignition V8 engine.

Engine S/N 002 was built with additional instrumentation to measure turbine and compressor clearance as a function of speed. Testing was initiated and a maximum speed of 81,000 rpm was achieved prior to instrumentation degradation and an engine oil leak.

Approximately 70 hours have been accumulated on S/N 001 and S/N 002 with 100 starts to date.

1.2 Compressor Development

Based on Test 1 data and subsequent analysis, the impeller and diffuser were modified to

restore deficiencies noted during Test 1 (ie, low flow and pressure ratio). The modifications included impeller tip diameter and inducer shroud line increase, increased vane height in the first diffuser row converging to the existing vane height of rows two and three, and stationary shroud contour modifications to accommodate impeller and diffuser modiciations. Hardware was fabricated and test rig build was initiated.

1.3 Turbine

Testing was initiated on the ceramic design hardware (fabricated in metal). Preliminary results indicate excellent stage performance at idle conditions.

Fabrication of the dual alloy turbine rotor for operation at 2100°F TIT was completed. Five rotors were successfully HIP bonded; four of these are for evaluation of mechanical properties and one for spin test and potential power section testing. Evaluation of the bond joint between the MAR-M 247 blade ring and powdered metal Astroloy hub indicated excellent integrity.

1.4 Combustion

Fuel nozzle development for the AGT101 2500°F configuration has been initiated with very encouraging results. Element screening tests were conducted using CO_2 injection to define mixing qualities and laser Doppler velocimeter (LDV) testing to map flow field velocities. Information from these tests was correlated with analytical results and aided in defining configurations for hot test evaluation.

Emission testing was conducted at adjusted flow conditions to yield the same pressure drop and fuel-air ratios for AGT101 (2500°F) testing. Inlet temperature was held at 1600°F and correlations established based on NASA TM81640 data for residence time and temperature. Data indicates that the program emission goals are achievable.

1.5 Ceramic Component Development

Multiple ceramic component deliveries and evaluations have been accomplished. Thermal screening tests have been conducted on 10 components (4 shrouds, 2 combustor baffles, 2 stator sets, and 2 transition ducts). During these tests, two turbine shrouds, later judged to be of marginal quality, fractured as a result of thermal conditions. All other components successfully passed a minimum of five 1600°F light off cycles.

Rotor development was highlighted with multiple spin testing of one ACC bladed rotor to 83,000 rpm, with minor blade damage, and subsequently to 95,400 rpm (95.4 percent design speed) before fracturing at a surface initated origin.

2.0 INTRODUCTION

This report is the fifth in a series of Semi-annual Technical Summary Reports for the Advanced Gas Turbine (AGT) Powertrain System Development Project, authorized under NASA Contract DEN3-167 and sponsored by the Department of Energy. This report has been prepared by The Garrett Turbine Engine Company (hereinafter referred to as Garrett), a Division of The Garrett Corporation, and includes information provided by Ford Motor Company, The Carborundum Company, and AiResearch Casting Company. The project is administered by Mr. Roger Palmer, Project Manager, NASA-Lewis Research Center, Cleveland, Ohio. This report presents plans and progress from January 1982 through June 1982.

Project effort conducted under this contract is part of the DOE Gas Turbine Highway Vehicle System Program. This program is oriented at providing the United States automotive industry the high-risk long-range technology necessary to produce gas turbine powertrains for automobiles that will have reduced fuel consumption and reduced environmental impact. It is intended that technology resulting from this program be capable of reaching the marketplace by the early 1990's.

The advanced automotive gas turbine, when installed in a Ford vehicle (3000 pounds inertia weight) would provide:

- A CFDC fuel economy of 42.8 miles per gallon based on Environmental Protection Agency (EPA) test procedures and Diesel No. 2 fuel. The AGT-powered vehicle will give substantially the same overall vehicle driveability and performance as a comparable production vehicle powered by a conventional spark-ignition powertrain system
- Emissions less than federal standards
- Ability to use a variety of fuels

The Garrett/Ford Advanced Automotive Gas Turbine has been designated the AGT101. The AGT101 includes ceramic parts in its ultimate configuration. The program was initiated in October 1979 and was to entail 68 months. Two phases were planned; Phase I was 45 months long and Phase II was 23 months. Phase I was to involve most of the component/ceramic technology effort and the early engine and vehicle testing. Phase II was scheduled to include completion of the all ceramic engine effort plus the vehicle deliveries and evaluation.

Budget reductions in mid FY 1981 have resulted in a reorientation of the program. The vehicle, transmission and engine gearbox/transmission effort have been deferred indefinitely. The program is now oriented toward developing the long-range high-risk technology of the AGT101 gas turbine such that the auto industry can carry that technology forward to production in the 1990's. Emphasis on ceramics, gas bearings, low emission combustion and improved component performance continue. The AGT101 gas turbine is being used as a test bed in which to develop these technologies.

Since FY 1982 and subsequent year funding is not defined, the actual program details are also not defined. Garrett and Ford have suggested that the technology work be continued through FY 1985, culminating in the demonstration of the original goals of engine specific fuel consumption, power output, and emissions. In addition, the viability of ceramics will have been demonstrated in the AGT101 test bed and the potential of economically producing the ceramic parts in automotive production quantities will have been assessed by Ford. When these goals are achieved, Ford will be in a position to proceed, without Government support through the typical preproduction tasks which could then lead to production in the 1990's.

The primary technology challenges in the program continue to be the development of the ceramic components and related high-

performance gas turbine aerothermodynamic components for the AGT101. The AGT101 nominally is a 100 shp engine, capable of speeds to 100,000 rpm and operating at turbine inlet temperatures to 2500°F. Specific fuel consumption is less than 0.3 over much of the operating range.

This report is structured to initially review the power section effort conducted to date. This discussion is followed by a review of the component/ceramic technology development. Appendices include reports of progress from Ford, AiResearch Casting Company, and the Carborundum Company.

3.0 POWERTRAIN DEVELOPMENT

3.1 AGT101 Engine Test

Testing was continued on the S/N001, Build 4 engine which included fuel system modifications for improved fuel atomization and light-off characteristics. On January 5, 1982, the engine was successfully demonstrated for the House Science and Technology Committee visitors while operating at 53,000 rpm for over 2 hours. Testing was resumed after the demonstration at which time a speed variation and increased runout of the high speed ball bearing was observed. A partial engine disassembly revealed a small spall on one ball, otherwise the bearing appeared to be in excellent condition. The bearing was returned to the factory for further analysis.

The engine was reassembled with a new bearing and returned to the test cell on January 8, 1982.The full authority digital electronic control unit (ECU) was integrated with the power section to provide speed, temperature and starting control functions. Engine testing was continued with the ECU at speeds up to 63,500 rpm during which time an optimum fuel schedule and lean-blow-out (LBO) limit were established for the metallic engine. The excellent combustor LBO limit allowed the minimum fuel schedule to be reduced 20 percent from the original value.

A dead weight fuel measurement system was installed to provide an accurate fuel flow measurement in the idle flow range. The engine then was operated at speeds of 50,000, 60,000 and 70,000 rpm and loaded to 1600°F turbine inlet temperature. During this testing a slight variation was noticed in the regenerator speed. As engine speed was increased to 80,000 rpm, it was observed that the engine was not being controlled at a constant speed. Shortly thereafter the engine rapidly decelerated to zero speed.

Following shutdown, the regenerator core continued to operate by means of the hydraulic drive with visual and indicated speed variations accompanied by a squealing noise. At this time the engine had accumulated a total operating time of 40 hours.

A disassembly inspection of the engine showed that the turbine wheel was tightly frozen in position. Further inspection revealed the turbine shroud had settled downward approximately 0.030 inch relative to the axis of the foil gas bearing supporting the turbine. The heads of two of the three bolts supporting the turbine shroud also indicated movement relative to the original positions on the shroud.

The turbine wheel was pressed through the foil bearing and removed from the engine. The turbine foil bearing journal was damaged and manifested a buildup of foil material on the journal surface. The foils, while damaged beyond use, were intact and lightly bonded together.

Measurement of the eccentricity between the turbine shroud and foil bearing carrier indicated 0.065 inch total indicator reading (TIR) confirming the approximate measurements made earlier.

Two of the three bolts supporting the turbine shroud were bent. All other components of AGT101 S/N 001 were undamaged.

Analysis of the evidence clearly indicated that the heads of the three bolts supporting the turbine shroud had not slipped in the radial shroud slots as intended during the thermal expansion of the turbine shroud. As a result the turbine shroud was forced eccentric to the axis of rotation and caused contact between the wheel and shroud at the one o'clock position. Due to the resilience in the foil bearing, the engine continued to run as the shroud increasingly forced the wheel to displace thus reducing the foil bearing sway space. When rotor deflection in the foil bearing had consumed the available sway space, a bearing overload occurred and the bearing failed, rapidly stopping the rotor.

Inspection of the hydraulic system used to drive the regenerator during the last series of tests, indicated that the pressure relief had been set too low (800 psi). As the regenerator drive load increased, the drive pressure increased until the relief pressure was reached, at which time regenerator speed could not be maintained.

A redesign of the turbine support system was initiated. The design features a radial flexure system consisting of nine beams supporting the turbine shroud as shown in Figure 1.

The AGT101 S/N 001 was assembled (Build 5) with the redesigned turbine shroud support system components. Installation of proximity instrumentation on the turbine shroud was to permit monitoring relative motion and clearance between the turbine wheel and shroud. Two proximity probes, 180 degrees apart, were mounted on the turbine shroud in the turbine exducer area. Displacement probe positions are shown in Figure 2. The engine was installed in the test cell on March 30, 1982 and subsequently completed 30 start/stop cycles of hot testing to verify the ability of the redesigned turbine shroud support structure to maintain shroud to turbine rotor concentricity during engine operation and after shutdown and cooling. The tests were successfully conducted and the turbine shroud did not vary in the radial direction, relative to the rotor. Each start/stop cycle required approximately 45 minutes to achieve the full range of temperatures between 200 and 1250°F on the shroud support system. Maximum rotor speed for each cycle was 50,000 rpm.

Thermal soak-back tests also were conducted on the Build 5 engine from 1448°F TIT shutdown temperatures. The purpose of these tests was to determine the foil bearing temperatures as a result of soak-back. The maximum temperature on the foils was 390°F. Peak thermal soak-back occurred 12 minutes after shutdown as predicted.

Additional testing was done to define rotating group behavior up to 75,000 rpm, power

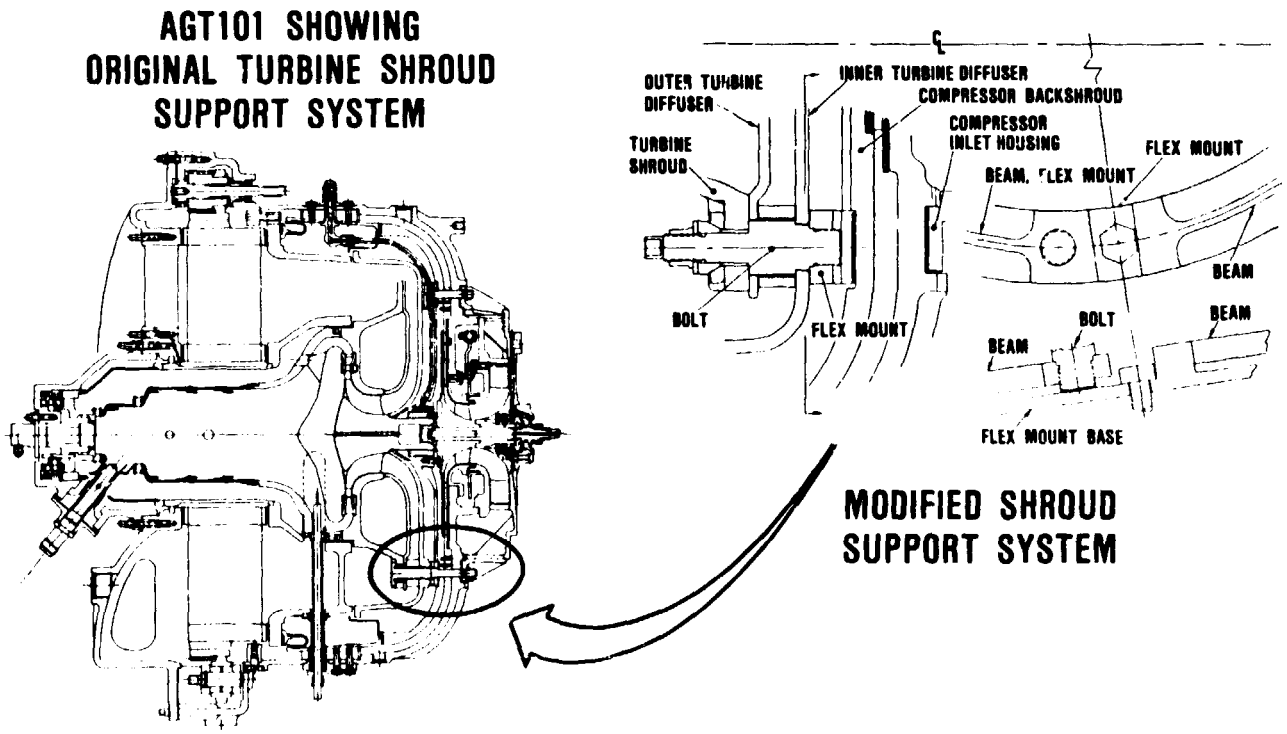

Figure 1. AGT101 Turbine Shroud Support System.

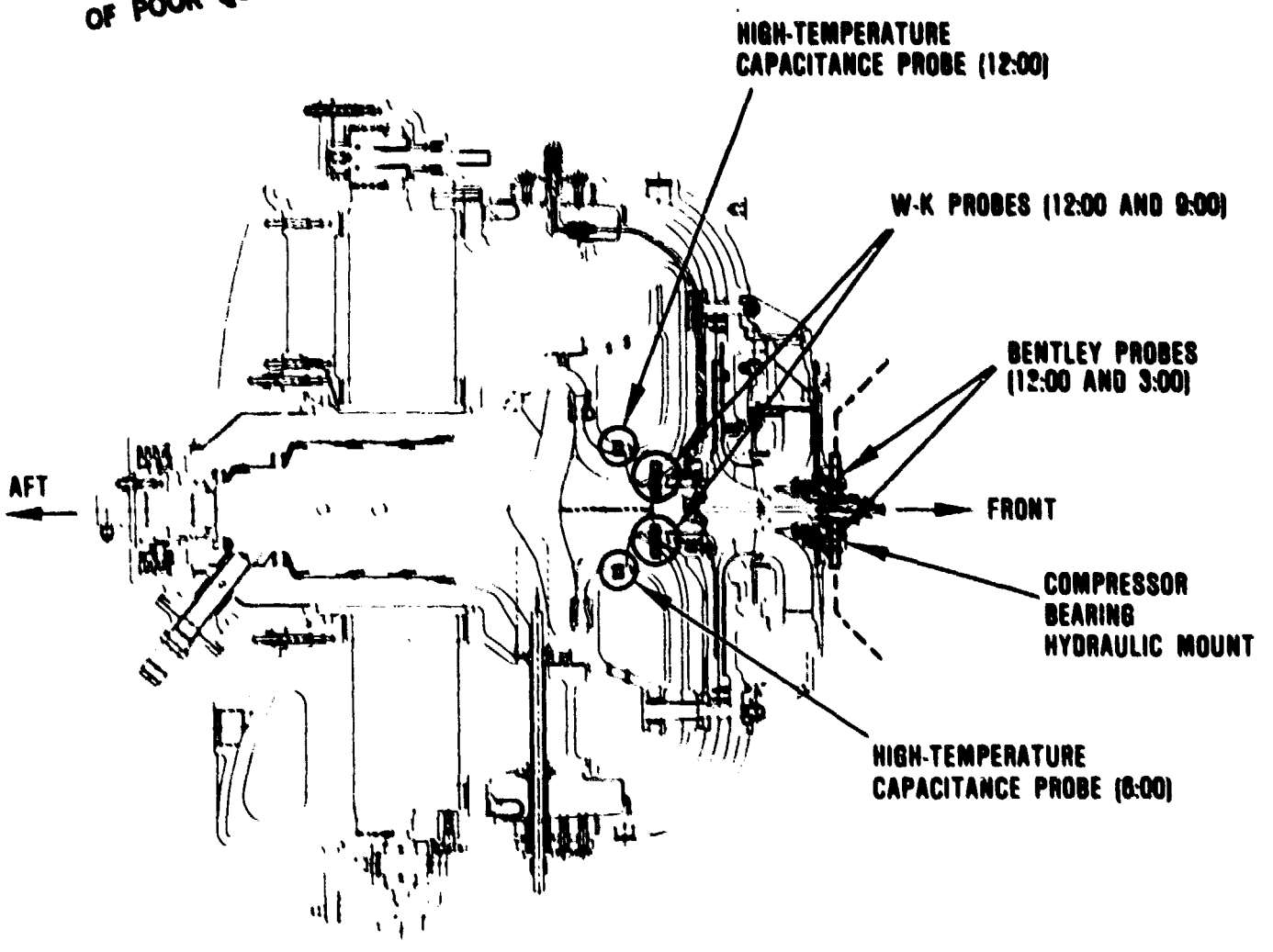

Figure 2. Displacement Probe Locations (Clock Positions are Referenced to Front of Engine).

output, foil bearing operation and idle speed fuel consumption.

Rotating group dynamic behavior was excellent throughout testing. One of the displacement probes ceased to function after about 11 hours of engine operation, which prevented monitoring the foil bearing journal motion during the remainder of testing.

Engine power was measured using a hydraulic dynamometer. Initially the power output was 5.7 bhp (uncorrected) at 75,000 rpm. This was lower than the 11 hp anticipated at 1600°F TIT with VIGVs open at 40 to 50 degrees.

A decision was made to go on to fuel consumption testing. The engine was extremely difficult to start and after shutdown would not restart. The failure to restart was traced to a buckled combustor. Investigation revealed the combustor buckled because of inadequate clearance between the combustor cap, heat-shield, and combustor spacer during operation. With modifications to increase clearance between parts as shown in Figure 3 and a new combustor, the engine restarted without any problems. After temperatures stabilized, it was noted that TIT was about 100 to 120°F lower than during previous running due to improved regenerator sealing.

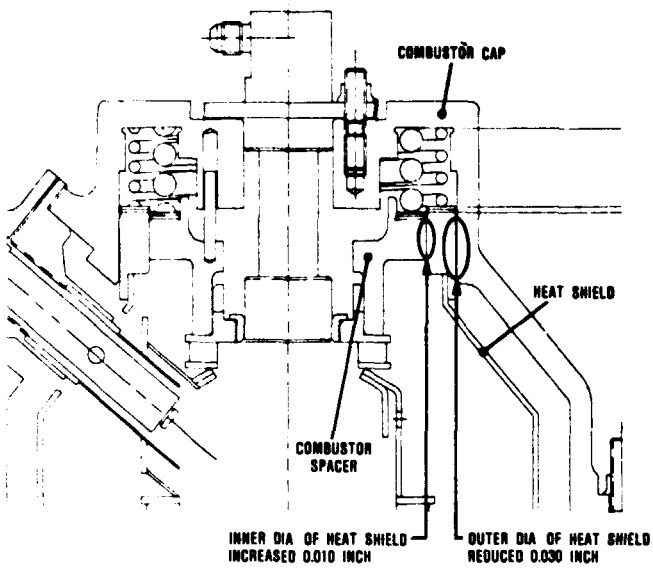

Figure 3. Changes to Combustor Heat Shield and Spacer to Avoid Thermally Induced Seizure.

Engine power was measured again at 75,000 rpm and power output was 8 bhp with VIGVs open at 40 to 50-degrees and a 1600°F TIT. This was recorded as the best output attainable with the current level of regenerator seal leakage. Engine idle fuel consumption was measured at 2.6 lbs/hr.

The engine was removed from the test cell and returned to the assembly area for partial inspection and teardown. Inspection of the regenerator section revealed no abnormalities.

The S/N 002 engine was assembled with the turbine shroud support modifications that were incorporated in the S/N 001 engine to maintain shroud concentricity with the turbine rotor. Additional instrumentation was installed to monitor both radial and axial clearances for the turbine and the compressor. Regenerator position probes and thermocouples for regenerator seal and turbine nozzle metal temperatures also were installed.

Initial testing of the S/N 002 engine commenced on May 14, 1982 and consisted of motoring and hot tests; conducted without incident. Further tests were made to map aerodynamic clearances over the operating speed range. Turbine clearance probe signals were intermittant following initial lightoff in the clearance tests but significant compressor axial clearance data were recorded up to an engine speed of 81,000 rpm. The engine was removed from the test cell after 4.6 hours and 23 starts due to degradation of the clearance and dynamic instrumentation and an apparent gearbox oil leak to the compressor inlet. The engine dynamic behavior indicated probably improper axial clearance of the hydraulic mount.

A teardown inspection revealed that sealing plugs were not installed in the oil and buffer air galleries of the inlet housing as specified by print. This allowed oil to leak into the compressor inlet. Insufficient hydraulic mount axial clearance was verified. The "wavy" spring loading the hydraulic dam was noted to bind on its OD, when compressed, preventing proper action of the dam. The assembly procedure was modified to reflect refined assembly and inspection techniques based on previous experience; for example, the hydraulic mount axial clearance was measured as a subassembly and verified again in the final assembly. After installing the plugs in the inlet housing and reducing the wavy spring OD for adequate clearance, reassembly (Build 1A) was initiated; testing of Build 1A is expected in July 1982.

A chronological summary of the tests conducted to date on the S/N 001 and S/N 002 engines and accumulated test hours is presented in Figure 4.

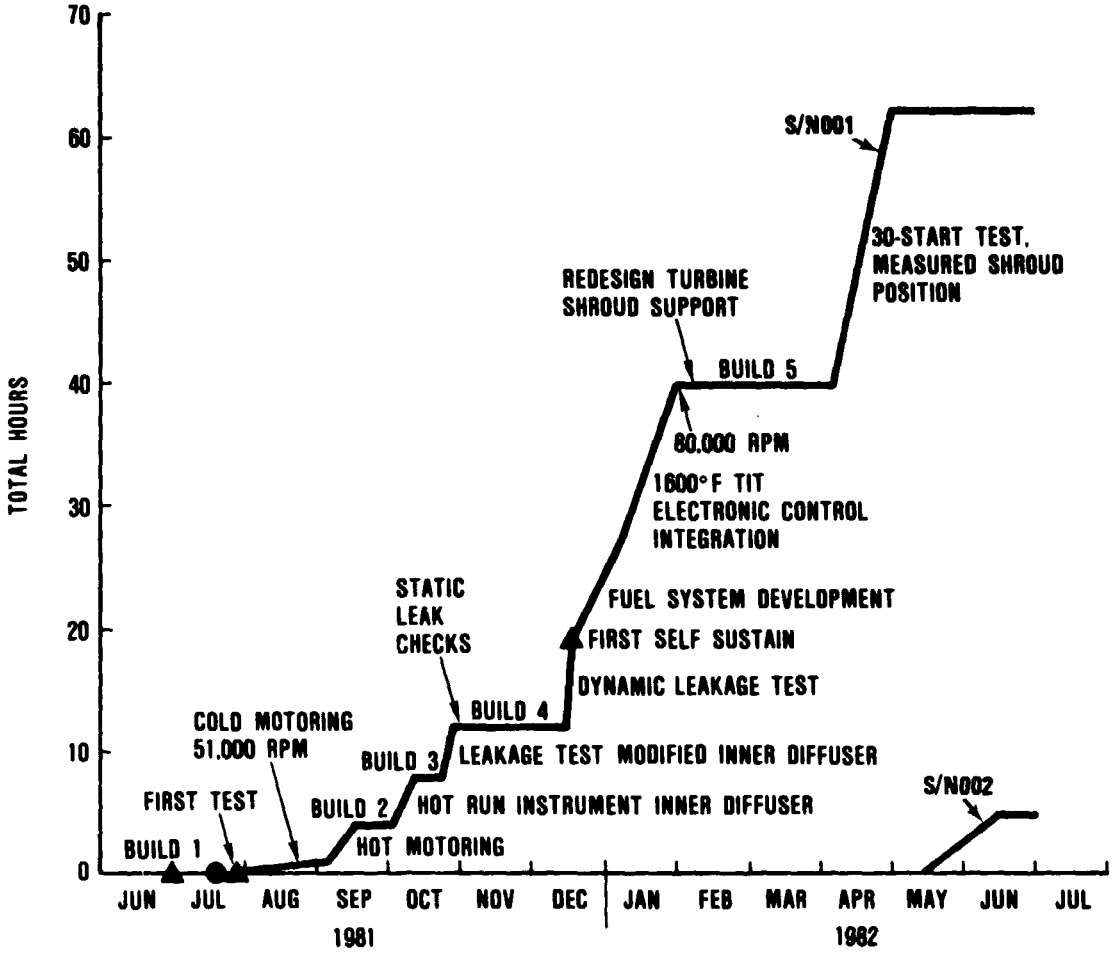

Figure 4. AGT101 Test Chronology.

4.0 COMPONENT/SUBSYSTEM DEVELOPMENT

Component/Subsystem development activities during this reporting period were concentrated on support of AGT101 1600°F engine testing, continuation of ceramic development activities, continued fuel nozzle development for the AGT101 2500°F engine, hardware procurement for modified compressor test and preparation for AGT101 2500°F cold turbine aerodynamic testing. Figures 5 shows the performance rating stations for the AGT101 engine and components.

The following sections discuss major efforts and accomplishments during the reporting period for each component/subsystem.

4.1 Compressor

As stated in Reference 4, the AGT101 Test 1 compressor stage was below design flow and pressure ratio. Therefore, a modification of the baseline stage design was instituted, based on Test 1 data and subsequent analysis. Activ-

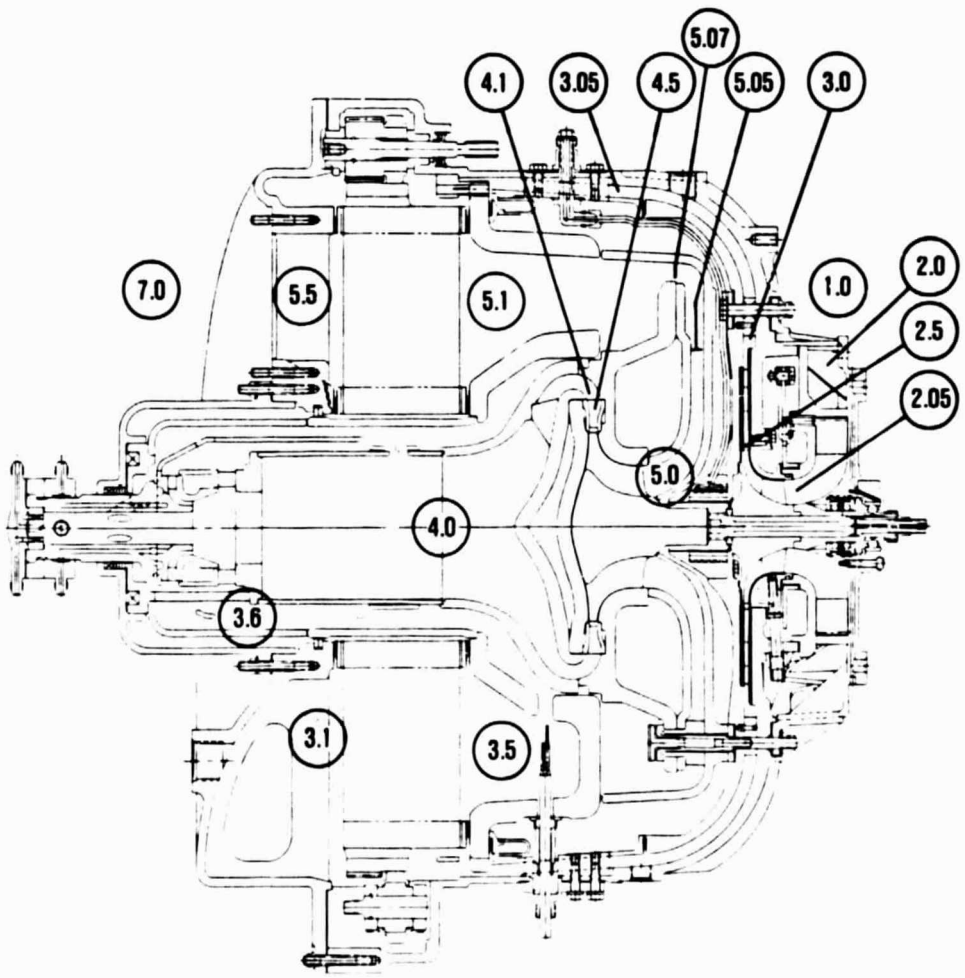

Figure 5. Performance Rating Stations.

ities during this reporting period concentrated on design and procurement of the modified impeller and diffuser for Test 2.

4.1.1 Design Modification

Based on initial test data, the impeller was found to be low on work input and flow capacity. To restore these deficiencies back to design levels, an analysis was conducted to evaluate several exclusive and related modifications. Working within available hardware constraints, modifications that added 0.052 inch to the impeller tip radius, 0.48 inch to the inducer shroud line and 0.018 inch to the exit blade height were analyzed to increase flow capacity and work. A comparison of the modified impeller blade loadings and loadings based on Test 1 data is shown in Figures 6 and 7 for the shroud and hub respectively. The loadings shown for this Test 1 impeller were modeled using tested losses and deviation. Figure 8 shows the modified impeller geometry.

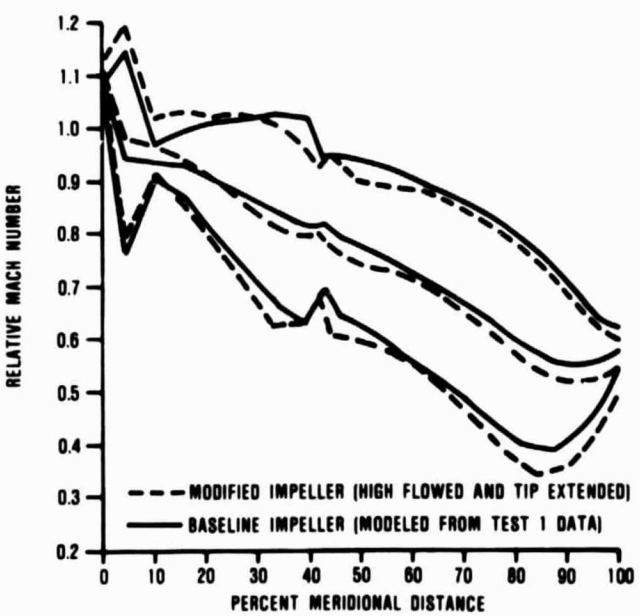

Figure 6. AGT101 Modified Impeller Blade Loadings--Tip.

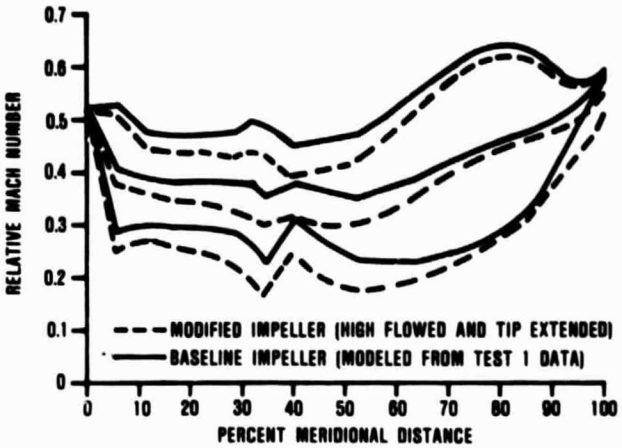

Figure 7. AGT101 Modified Impeller Blade Loadings--Hub.

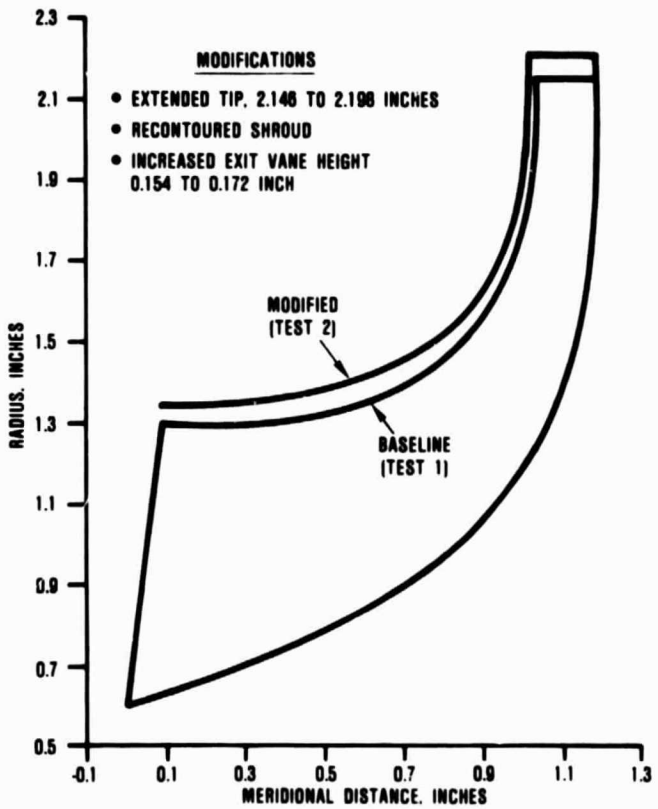

Figure 8. AGT101 Modified Impeller Geometry.

Based on the modified impeller geometries, the stationary shroud and diffuser also were modified. Since Test 1 data indicated that the diffuser minimum loss occurred at design incidence, the original diffuser design criteria was retained. In addition, since the match obtained between vane rows 1, 2, and 3 showed good performance, a decision was made to modify only the 1st vane row to accommodate the larger impeller and retain the 2nd and 3rd vane geometries as designed and tested. To accomplish this, vane row 1 was increased in height, and the vane height was linearly converged to match vane row 2. At the close of the reporting period, all hardware has been fabricated and instrumented, and build of the rig initiated. Initial testing will be conducted without the diffuser, and with IGVs locked in the 0 degree position, to assess the modified impeller characteristics (flow and work). Full stage testing will be conducted following vaneless diffuser testing.

4.2 Turbine

Activities for turbine component development entailed preparation for AGT101 ceramic design cold turbine aerodynamic performance mapping, build and installation of the test rig in the test facility and fabrication of dual allow turbine rotors.

4.2.1 Cold Air Turbine Testing

As stated in Reference 3, the cold air turbine test program was modified to support AGT101 1600°F engine development, with test of the ceramic design to follow. Therefore, in preparation for testing, all rig hardware was inspected and refurbished where necessary. The instrumentation was checked and repaired as required. The unit was assembled and installed in the test facility. At the close of the reporting period testing had been initiated. Results will be presented during the next reporting period.

4.3 AGT101 Mod I Dual Alloy Turbine Rotor Fabrication

The turbine inlet temperature for AGT101 (2100°F) engine development imposes unique materials requirements for the turbine rotor fabrication. One material cannot satisfy all mechanical properties requirements. The limiting conditions for airfoils are stress rupture and creep, and tensile strength and hub low cycle fatigue.

Rather than compromise the turbine temperature capability and performance, a materials mix or dual alloy fabrication concept for the radial turbine wheel was preferred. Materials selected for the dual alloy wheel (DAW) fabrication are a cast MAR-M 247 bladed ring with directionally solidified (DS) inducer blade tips for higher temperature capability and powder metallurgy (PM) Astroloy for hub construction. The mated hub blade ring geometry is shown in Figure 9. The nominal chemical compositions of the materials are listed in Table 1.

4.3.1 Dual Alloy Wheel Assembly

The Astroloy was purchased as HIP powder consolidated logs. The TRW Prototype Foundry developed the DS blading casting technique as previously reported in Reference 2.

The hubs and bladed rings were machined as mated pairs to a 5-degree tapered fit

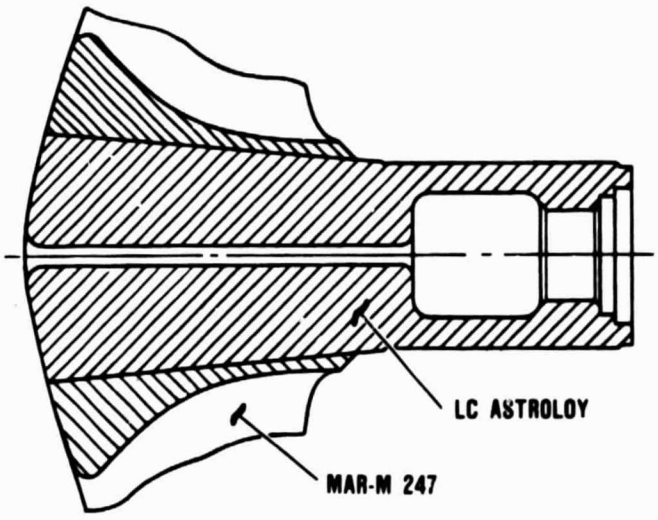

Figure 9. Dual Alloy Hub/Bladed Ring Assembly Cross Section.

TABLE 1. CHEMICAL COMPOSITIONS OF P/M ASTROLOY AND MAR-M 247

	C	Co	Cr	Mo	W	Ta	Al	Ti	B	Zr	Hf	Ni
PM Astroloy	0.02-0.004	17.0	15.0	5.0	-	-	4.0	3.5	0.025	0.06	-	Bal
Cast MAR-M 247	0.16	10.0	8.2	0.6	10.0	3.0	5.5	1.0	0.02	0.09	1.5	Bal

(Figure 9). Borazon (cubic BN) grinding wheels were used to arrive at a surface finish, typically about RMS 62 (Figures 10 and 11). Past experience at Garrett shows that the use of other grinding wheel compositions (ie, Al_2O_3 or SiC) results in foreign particles becoming imbedded in the work surfaces.

Exposed edges of mated assemblies were brush nickel plated (0.0002-0.0004 inch) and all parts were then cleaned using Garrett developed procedures. These include a sequence of steps starting with vapor degreasing followed by MEK solvent, HCl solution, distilled water, and Freon rinses. The mated assemblies were hermetically sealed using a vacuum brazing technique.

The first batch of five DAW assemblies were diffusion bonded during exposure to a

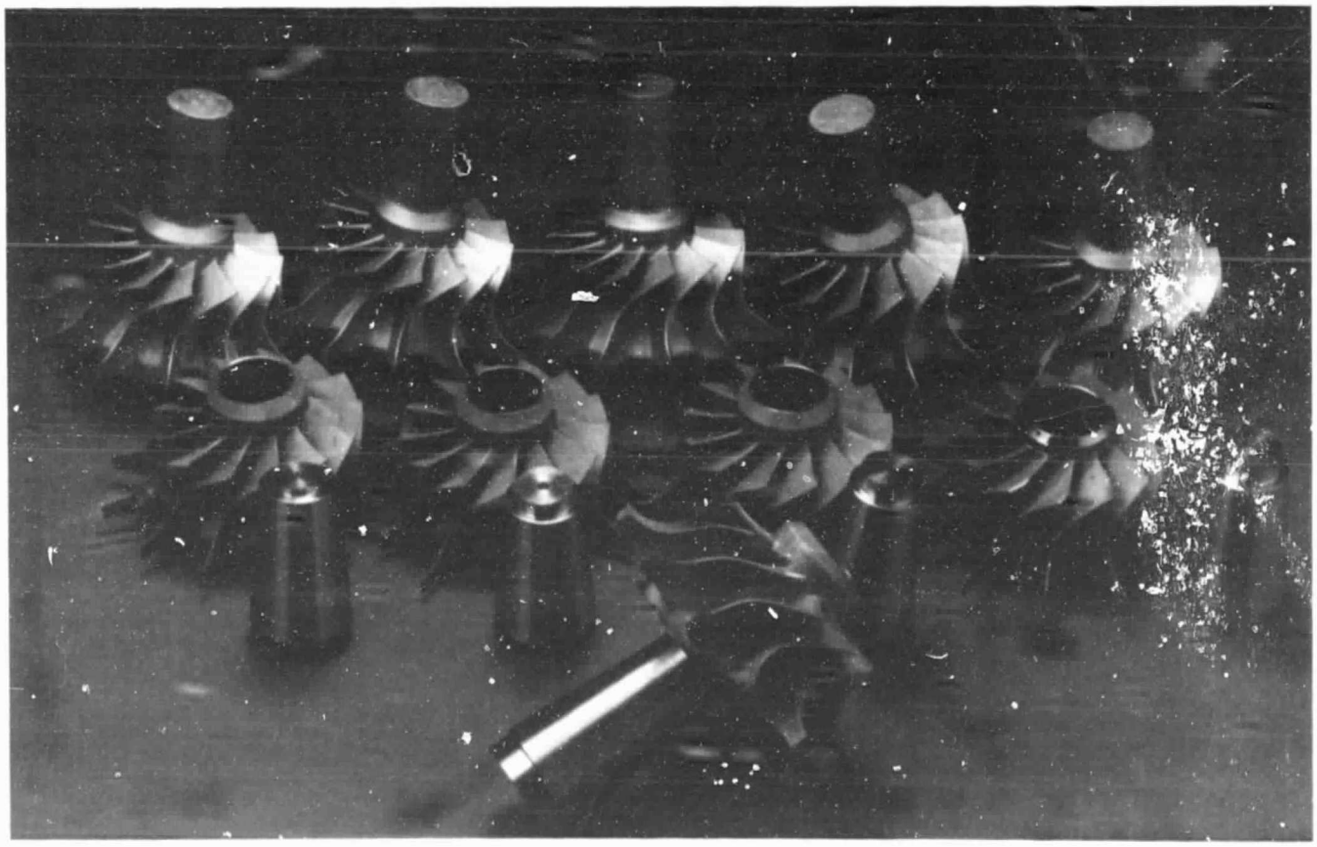

Figure 10. As-Cast AGT101 Bladed Rings and Machined Dual Alloy Wheel Assemblies.

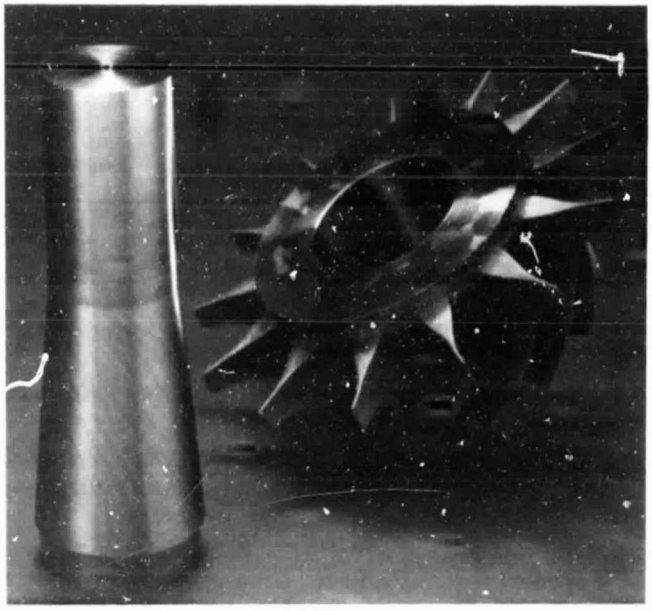

Figure 11. Machined AGT101 Dual Alloy Wheel Assembly--PM LC Astroloy Hub and MAR-M 247 Bladed Ring.

HIP cycle (2200 ±25°F/4 hrs/15 ksi) at the Howmet Turbine Components Corporation facilities (Figure 12). After bonding, all five assemblies were heat treated using the following standard Yo-Yo procedure developed for LC Astroloy:

Solution	1975°F/4 hrs/rapid argon cool
plus	1600°F/8 hrs/AC
	1800°F/4 hrs/AC
	1200°F/24 hrs/AC
	1400°F/8 hrs/AC

4.3.2 Bond Zone Evaluation

A representative macroetched cross-section of an AGT101 DAW, shown in Figure 13, indicates the presence of a continuous bond. Some braze alloy penetration is detected and a view of an unetched section of the bond zone shows the absence of porosity due to the Kirkendall effect or other causes (Figure 14). The area of braze penetration will be removed during final machining.

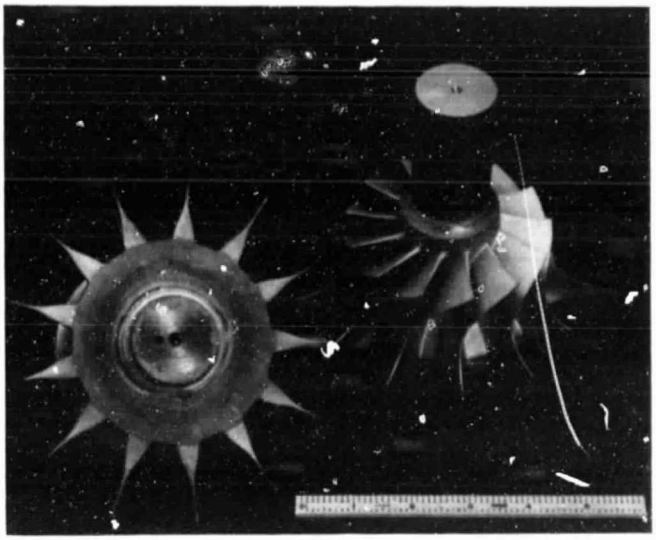

Figure 12. Dual Alloy Wheel Assemblies After Brazing and HIP Diffusion Bonding.

A great deal of diffusion across the bond zone is apparent (Figure 15); the γ' phase in the LC Astroloy is much finer than in the MAR-M 247 (Figure 16). The grain size in the LC Astroloy is unchanged when comparing as-received and bonded-heat treated material (Figures 15 and 17). However, coarse cooling γ' is present in the LC Astroloy grain bound-

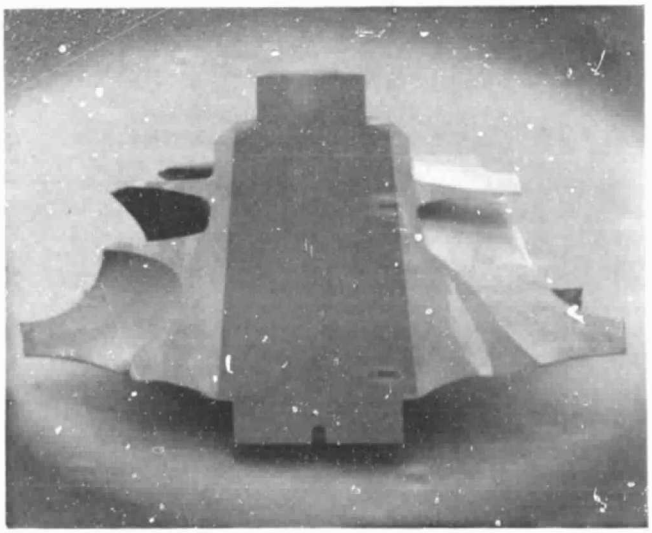

Figure 13. Microetched Cross Section of AGT101 Dual Alloy Wheel Test Specimen.

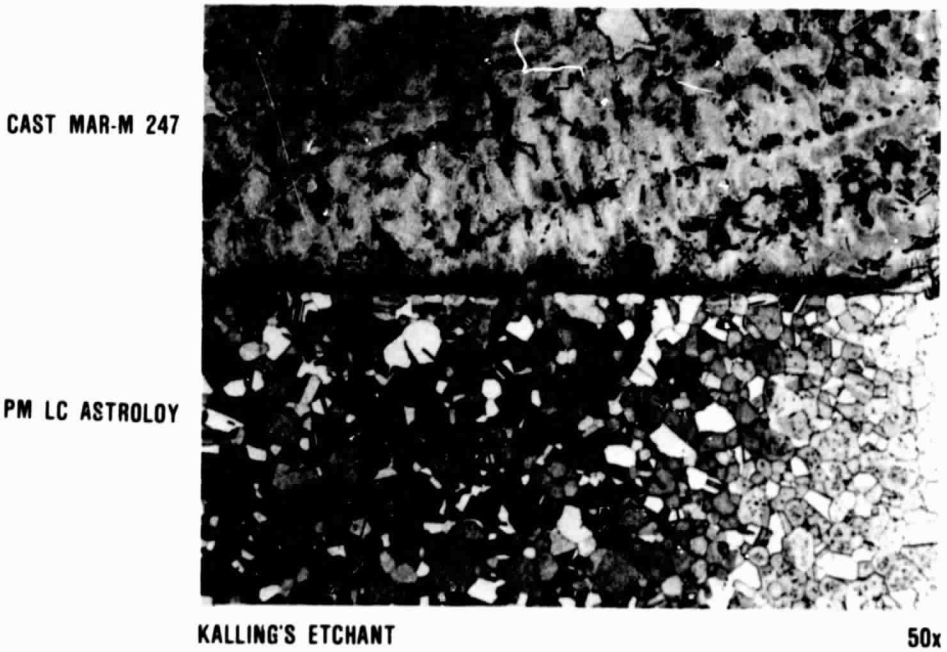

Figure 14. Braze Closure After HIP Diffusion Bonding (Sample was Subjected to Yo-Yo Heat Treatment).

PM LC ASTROLOY 400x

TYPICAL BOND ZONE 100x

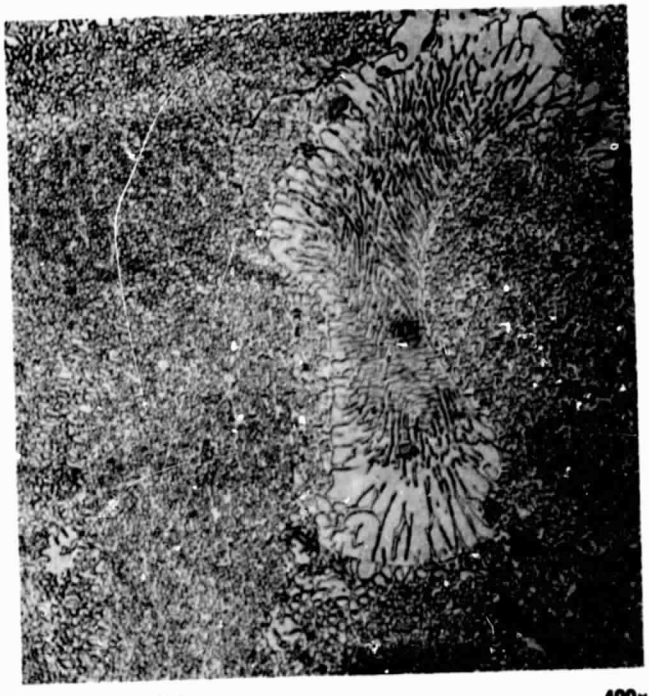

CAST MAR-M 247 400x

Figure 15. Diffusion Bonded PM LC Astroloy/Cast MAR-M 247 (Sample was Subjected to Yo-Yo Heat Treatment).

aries (Figure 17), and some coarse γ' is still observed in the LC Astroloy after processing (Figure 16).

An EDX spectrum analysis on both sides of the bond zone indicated a difference in relative intensity for Hf and W. The presence of Hf and W away from the bond zone and a Hf/W-rich phase in the LC Astroloy adjacent to the interface indicate that a great deal of interdiffusion across the bond zone did take place (Figure 18). The nascent LC Astroloy composition does not contain Hf or W. The micrographs in Figure 19 show that, in addition to interdiffusion, grain growth across the bond zone is very prominent.

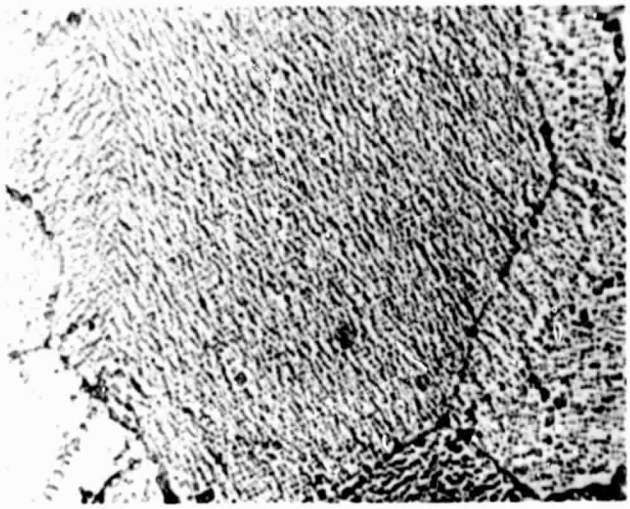

PM LC ASTROLOY 1000x

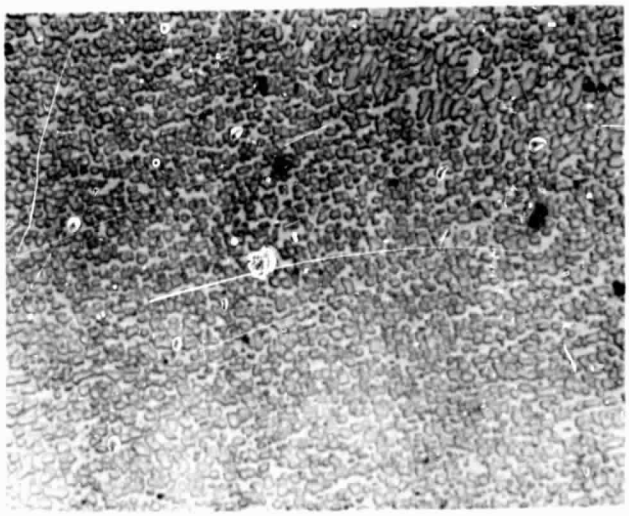

CAST MAR-M 247 1000x

Figure 16. Parent Metals for Dual Alloy Turbine Wheel Construction After Being Subjected to HIP and Yo-Yo Heat Treatment Cycles (Kalling's Etchant).

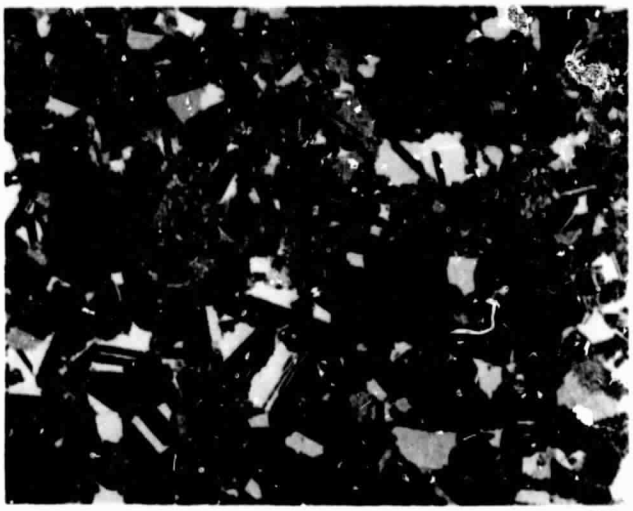

UNETCHED 100x

KALLING'S ETCHANT 1000x

Figure 17. As-HIPped PM LC Astroloy.

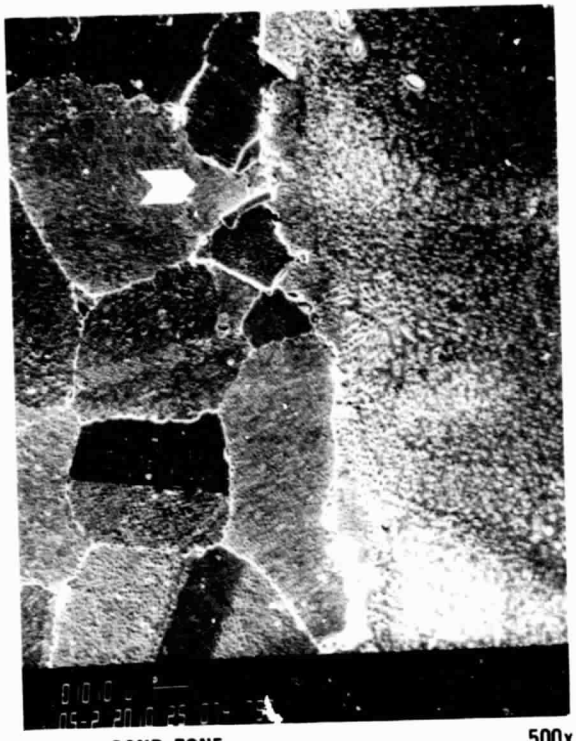

TYPICAL BOND ZONE 500x

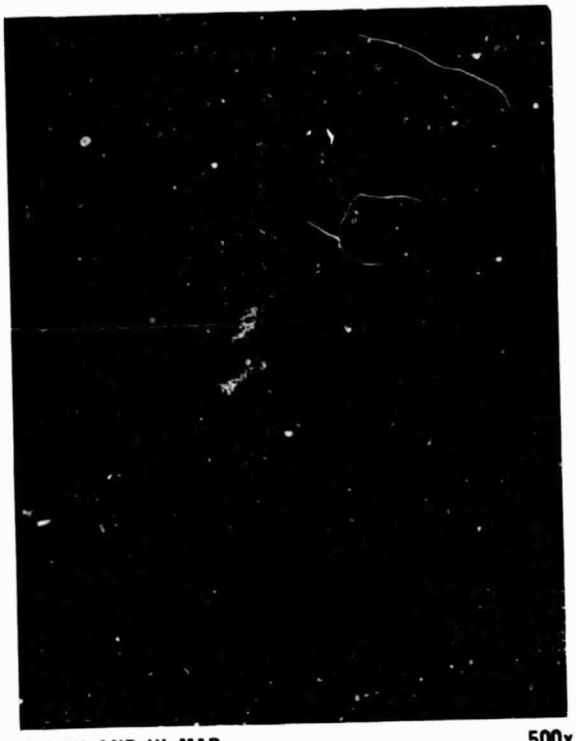

EDX Hf AND W MAP 500x

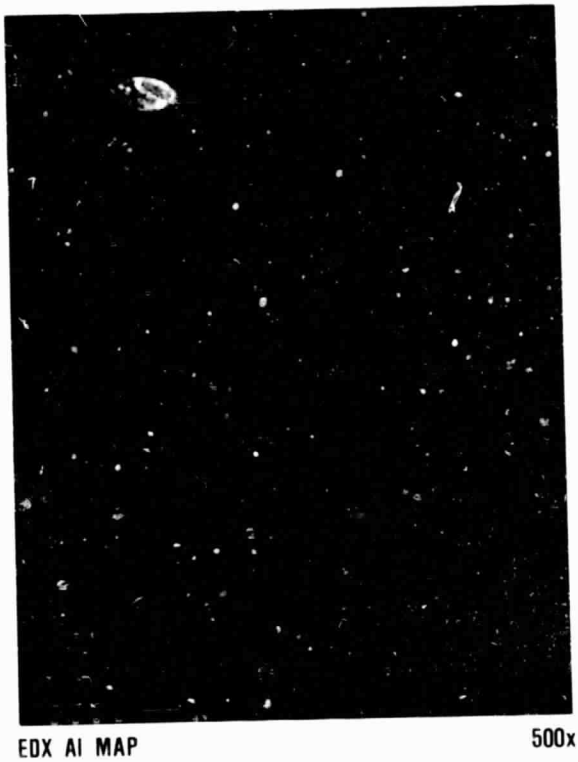

EDX Al MAP 500x

Figure 18. Diffusion Bonded PM LC Astroloy/Cast MAR-M 247 (Mapped Area Indicated by Arrow) (Sample After HIP Diffusion Bonding at 2200°F/4 Hours /15 KSI).

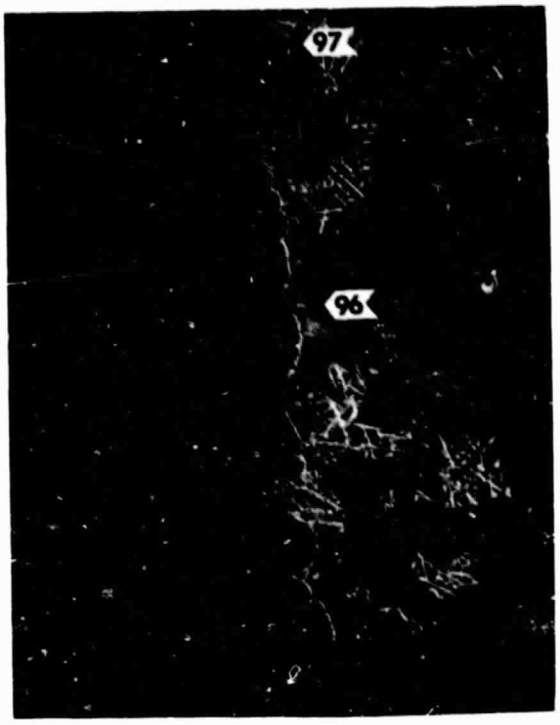

TYPICAL BOND ZONE 100x

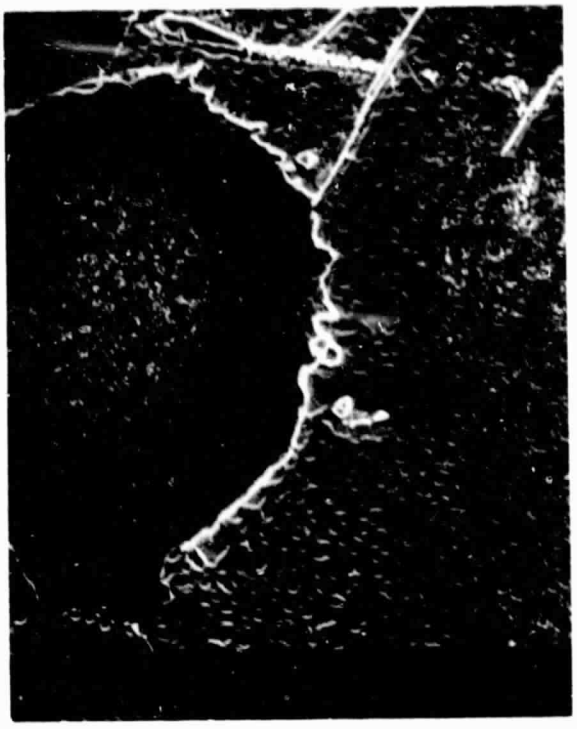

AREA 97 1000x

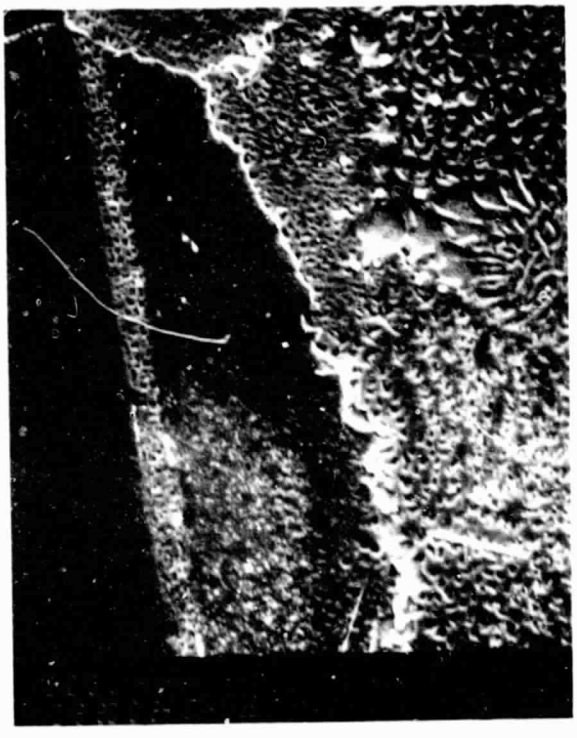

AREA 96 1000x

Figure 19. Diffusion Bonded PM LC Astroloy/Cast MAR-M 247 (Sample After HIP Diffusion Bonding at 2200°F/4 Hours/15 KSI and Yo-Yo Heat Treatment).

Based on preliminary observations, a satisfactory procedure has been developed at Garrett for fabricating dual alloy wheels for the AGT101 program. Of the five wheels processed, four are being used for destructive testing and one is being machined as a Mod I wheel for spin pit testing.

4.4 Combustion

The combustor development has proceeded along several parallel paths to define a configuration meeting Mod II emission goals and possess satisfactory structural durability. The subtasks can be divided into four basic areas: fuel nozzle development, element screening tests, analytical modeling of various configurations, and hot rig emission testing.

4.4.1 Fuel Nozzle Development

The major portion of the nozzle development was associated with the cold testing of the venturi nozzle described in Reference 4. The testing included both SMD (Sauter Mean Diameter) and patternator tests. The SMD testing characterized the droplet spray size as a function of operating conditions and the patternator tests assessed the fuel distribution within the spray cone. Various venturi configurations and fuel tube type as well as immersion depth were evaluated.

A schematic of the venturi fuel nozzle is shown in Figure 20. The modular design allowed the evaluation of a number of different configurations. Also, four different fuel injection techniques were evaluated:

- Cross-stream injection with a fuel-tube discharge orifice diameter of 0.010 inch
- Cross-stream with 0.069-inch diameter orifice
- Axial injection in the upstream direction with a 0.020-inch diameter orifice
- Axial injection downstream with a 0.020-inch diameter orifice

The best cross stream injection was obtained with the 0.069 inch orifice discharging at the wall of the throat and the best axial injection

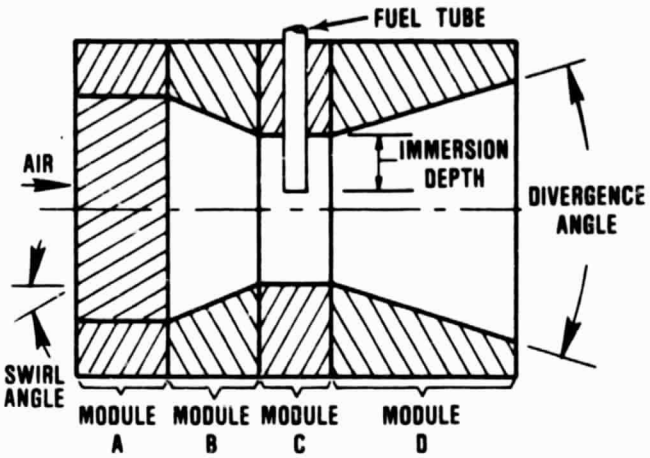

Figure 20. Venturi Fuel Nozzle.

was obtained when injected downstream. Both results were with zero swirl and a 15-degree divergence angle, although up to 15-degree swirl and a 34.4-degree divergence angle gave essentially the same atomization results. The 0-degree swirl and the 15-degree divergence angle gave the best distribution as represented in Figure 21 for 0-degree swirl.

The venturi nozzle data were correlated using several different expressions including Lefebvre thin sheet airblast atomizer and plain jet correlations and Jasuja's plain jet correlation. A comparison of the three correlations is shown in Figures 22 through 24; the best correlation was obtained with Jasuja's correlation. At this point the testing was terminated since the atomization characteristics of the venturi fuel nozzle did not show a marked improvement over the atomization of either the duplex or simplex nozzles.

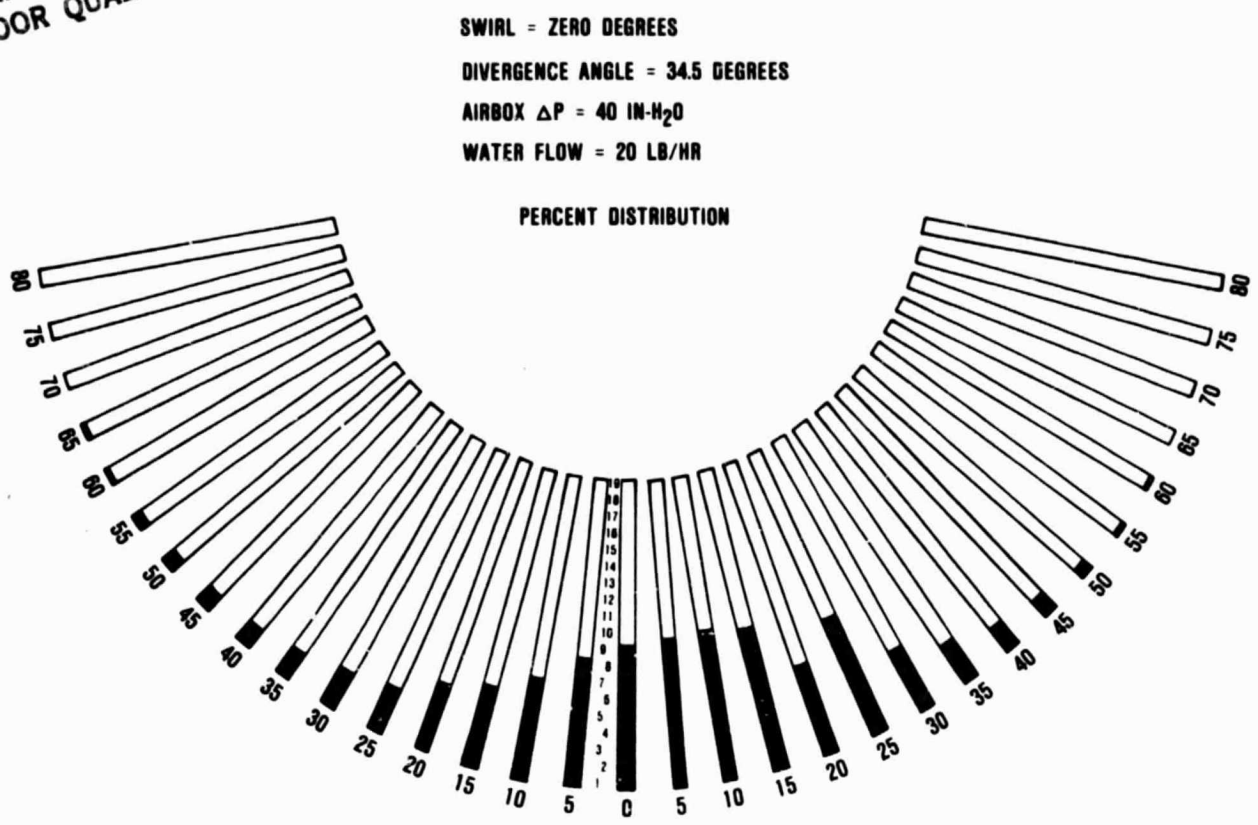

Figure 21. Venturi Fuel Nozzle Patternator Results.

4.4.2 Element Screening Tests

Two types of element screening test were conducted to provide flow field and mixing data and also to aid in selection of configurations to be hot tested. The data also were used for correlation with analytical models used to evaluate new designs. The first element testing discussed was LDV mapping of the flow field velocities for various configurations. The second mixing tests involved using carbon dioxide (CO_2) injected through the fuel nozzle fuel passages. The CO_2 concentrations then were measured downstream of the nozzle to establish fuel and air mixing.

4.4.2.1 LDV Measurements

The duplex fuel nozzle was mounted in the radial inflow swirler and installed in the cold flow rig. Air was pulled through the rig, by placing a vacuum on the discharge, and back scattering LDV measurements were taken to assess the axial and swirl velocities at various axial and radial locations. Four configurations were evaluated including combinations of the inner fuel nozzle swirler of 0 degree and 30 degrees and the radial inflow swirler one-half and full open. These same configurations and flow conditions then were modeled using the Garrett 2-D reacting flow model and a typical comparison for axial velocity at two axial stations is shown in Figures 25 and 26. The comparison shows that predicted radial diffusion was slower than was measured during test.

4.4.2.2 CO_2 Mixing Tests

The same cold flow rig used for LDV testing was used for CO_2 mixing tests. The rig was fitted with a single point axial and radial transversing probe. A rig schematic is shown

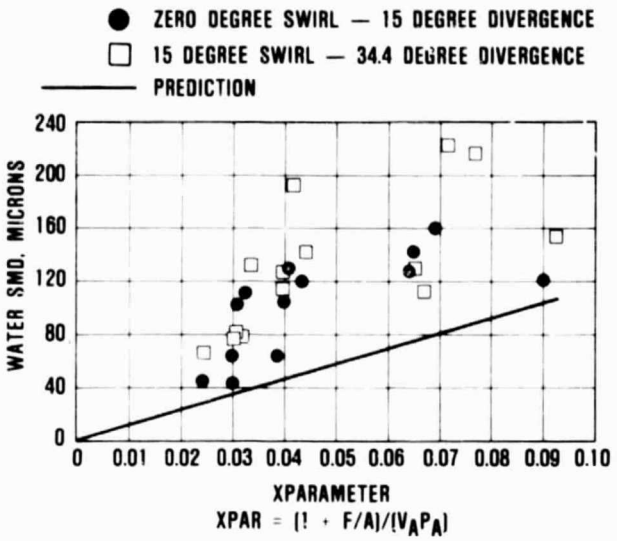

Figure 22. Comparison of Venturi Nozzle Measured SMD Data with Lefebvre Thin Sheet Airblast Atomized Correlation.

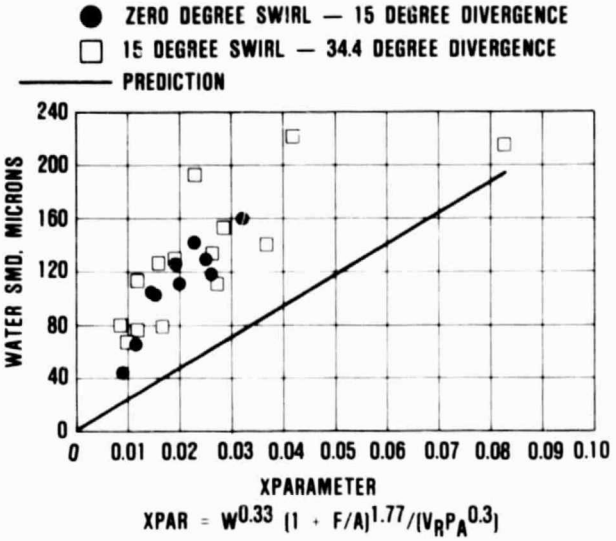

Figure 23. Comparison of Venturi Nozzle Measured SMD Data with Lefebvre Plain Jet Correlation.

in Figure 27. Testing was conducted for various pressure drops and configurations as given below:

- o Pressure drop - 2.3, 3.6, 5.2, and 7.3 percent
- o Radial inflow swirler - full open, one-half open, and closed
- o Nozzle inner swirler 0, 15, and 30 degrees
- o CO_2 injection - secondary, primary and both

A total of 25 test configurations were evaluated with eight radial positions and four axial positions for each configuration. The different effects noted from the test data were:

- o Higher pressure drop increased the nonuniformity
- o Decreasing the radial inflow swirler opening reduced the nonuniformity
- o Inner fuel nozzle swirler angle produced minimal effect

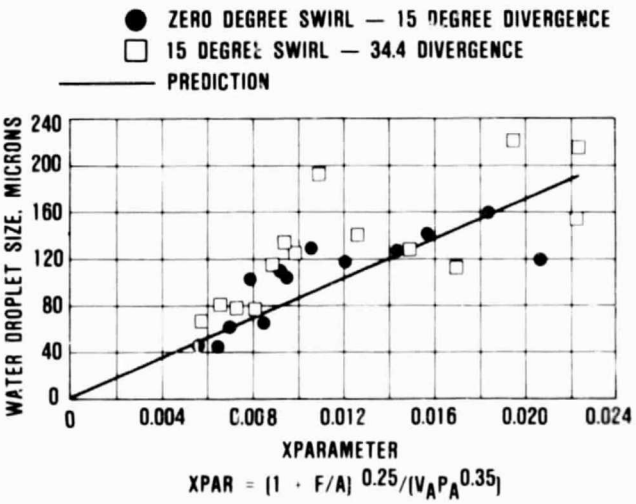

Figure 24. Comparison of Venturi Nozzle Measured SMD with Jasuja's Plain Jet Correlation.

- o Introducing fuel through the primary orifices increased the degree of non-mixing

As with the LDV data the 2-D model was used to predict CO_2 test data results. Figure 27

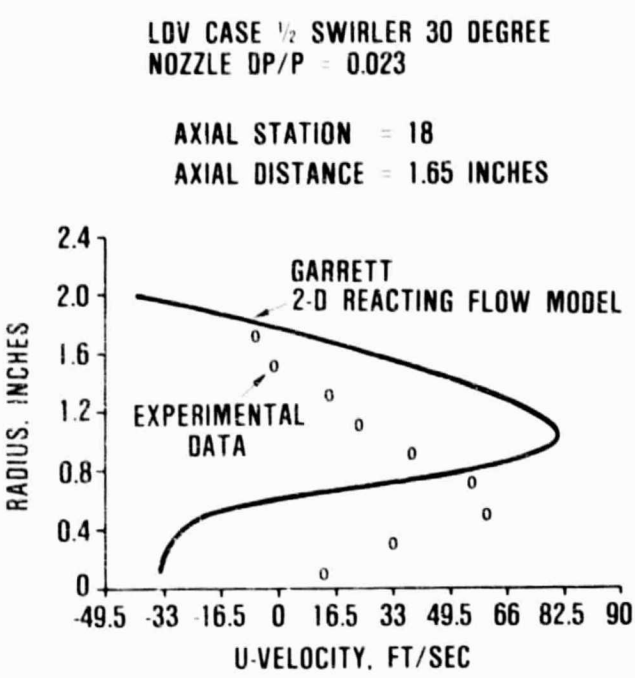

Figure 25. LDV Test Results.

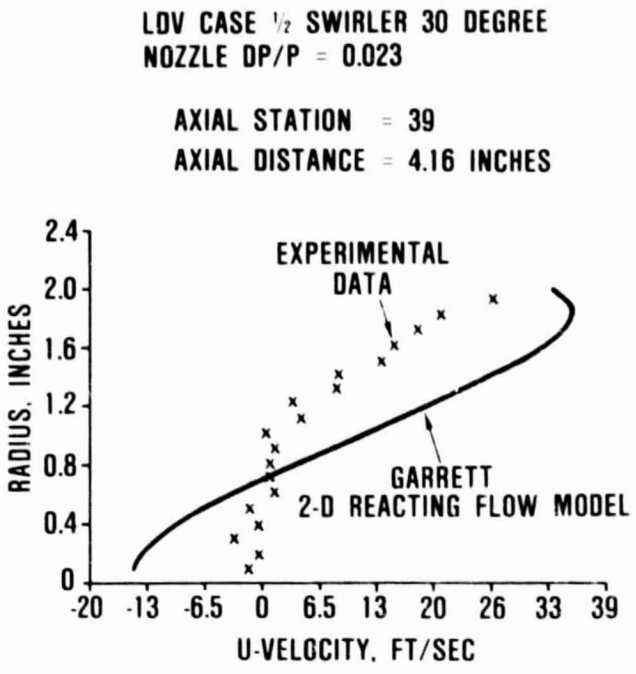

Figure 26. LDV Test Results.

also shows the measured and predicted radial profiles at various axial locations for one of the configurations. Again the model underpredicts the radial diffusion of the CO_2 resulting in more pronounced predicted CO_2 peaks. This data supports findings from the LDV comparisons and indicates that the predictions are more severe or a worse case when compared with the actual process.

4.4.3 Analytical Modeling

Following the comparison of 2-D model pre dictions with the LDV and CO_2 data, the model was used to evaluate other configurations that produced a more uniform distribution of fuel. A number of different geometries including different swirler and swirler combinations with and without primary or secondary holes were evaluated. The best configuration was a radial-axial swirler combination with the radial inflow swirler half open and the axial swirler located mid-way between the 2-inch cup diameter and the 4-inch diameter combustor. Figures 28 and 29 show the streamlines and temperature field respectively for a maximum power condition and Figures 30 and 31 depict an idle condition. For both power settings the flow field appears to be very uniform and therefore a design was initiated for a radial-axial swirler combination. Both swirlers were designed such that the area of each swirler can be independently changed to study the effect of various flow splits between the two swirlers.

4.4.4 Emission Testing

Emission testing was conducted using the same element rig used for the CO_2 mixing tests. Sampling was predominantly taken at a 6-inch axial location at 7 radial locations. A diagram of the rig in the cell is shown in Figure 32. Because the rig has less open area than the actual Mod II combustor, the inlet flow conditions were adjusted to yield the same pressure drop and fuel-air ratio as would be for the Mod II combustor inlet. Also the rig has been operated at a constant 1600°F inlet temperature and slightly reduced pressure to minimize stress on the rig. When a final configuration is arrived at, actual cycle conditions will be tested.

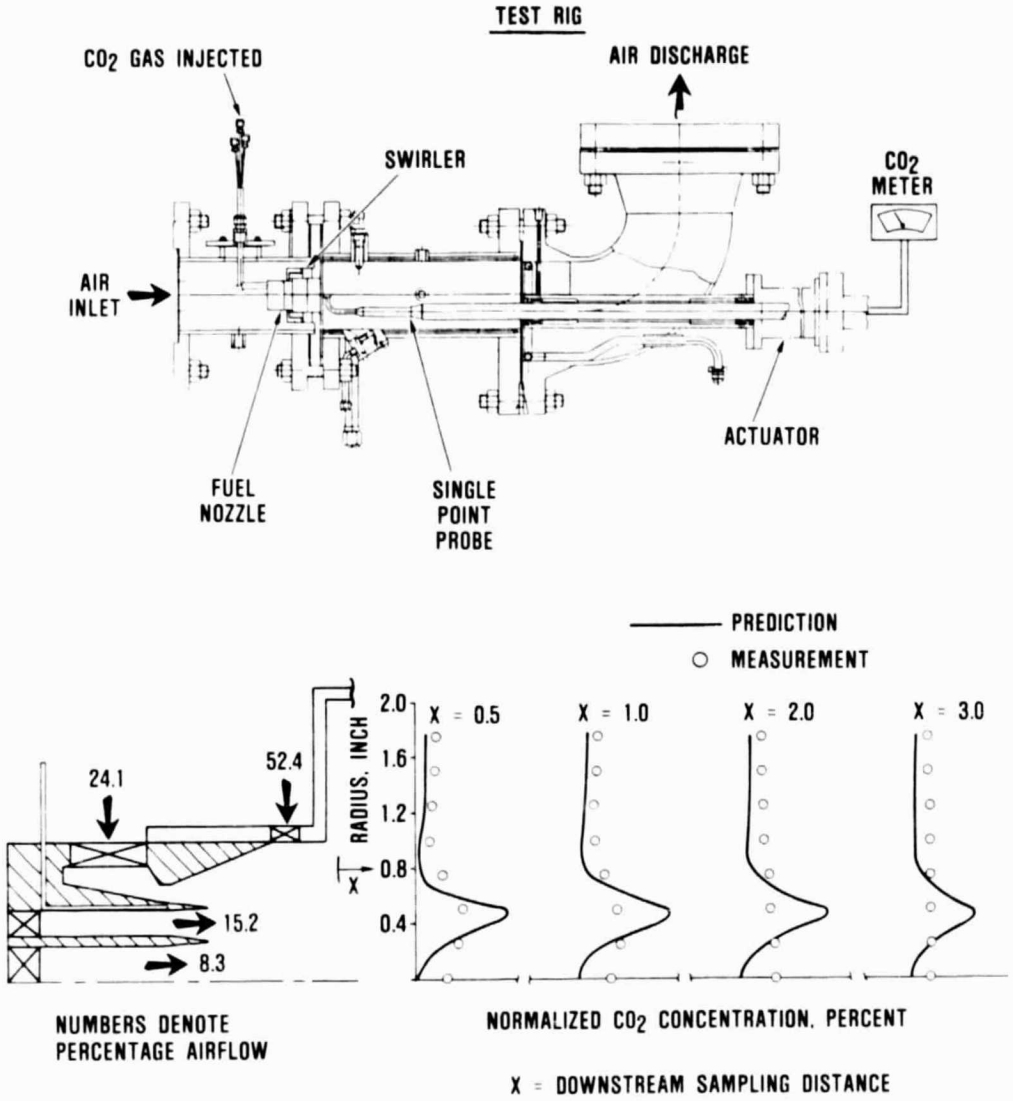

Figure 27. Mixing Test Rig and Data.

Initially the duplex fuel nozzle was used in testing; limited data were obtained prior to the development of an internal fuel leak. Testing was continued using the simplex fuel nozzle, which after several modifications produced good emission results even though there was a slight external fuel leak. The external leak has been repaired and testing will resume in July 1982.

The emission testing to date using the simplex nozzle is summarized in Table 2. Although some of the unburned hydrocarbon (HC) and CO were in excess of the goals, a reduction could be expected due to the higher inlet cycle temperature and the longer residence time associated with sampling at the engine exhaust plane. Such a correction was applied to the rig data using the information published in the Ultra-Lean Combustor Report (Reference 5). The results of the correction are shown in Figure 33. The effect of residence time was measured by taking emissions for a simulated maximum power 100 percent speed

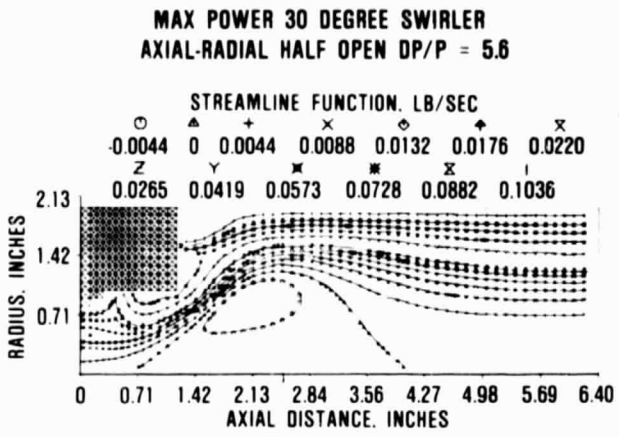

Figure 28. Predicted Streamlines for Maximum Power Condition.

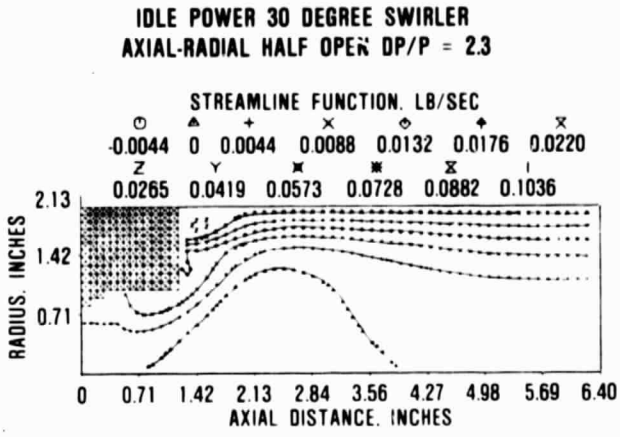

Figure 30. Predicted Streamlines for Idle Condition.

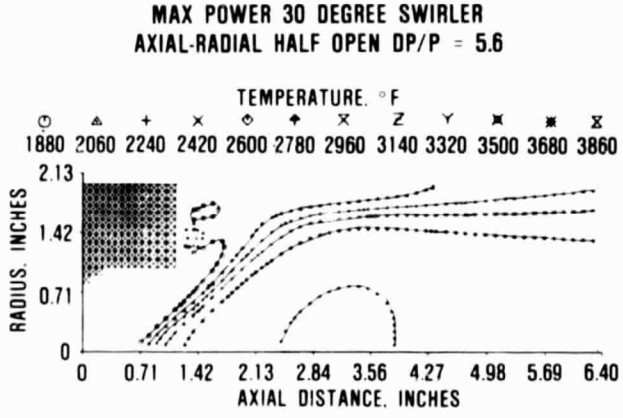

Figure 29. Predicted Temperature Field for Maximum Power Condition.

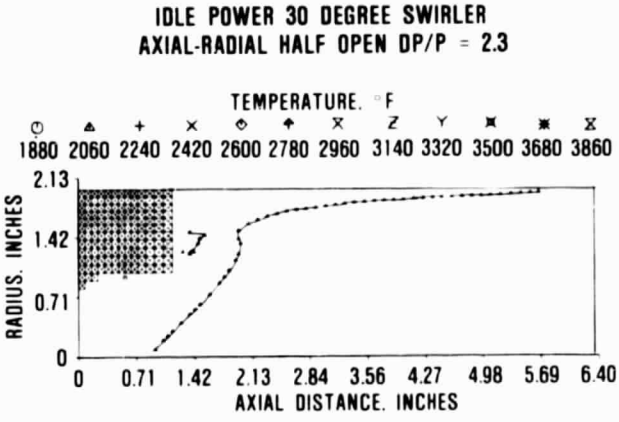

Figure 31. Predicted Temperature Field for for Idle Condition.

point at both the 3- and 6-inch location. The results are shown in Figure 34 and the drastic reduction in both HC and CO is evident between the two axial locations. Also of interest were that NO_x did not appreciably increase and the fuel-air ratio uniformity at the 3-inch location. The idle point was not shown since the information in Reference 5 did not present data at points similar to the idle conditions.

4.5 Regenerator

4.5.1 Ford Regenerator Development

The installation of a new induction heater system, which is required to bond the regenerator ring gear to the matrix, was completed during this report period. Three Corning thin-wall AS cores and one NGK thick-wall core were bonded and sent to Garrett.

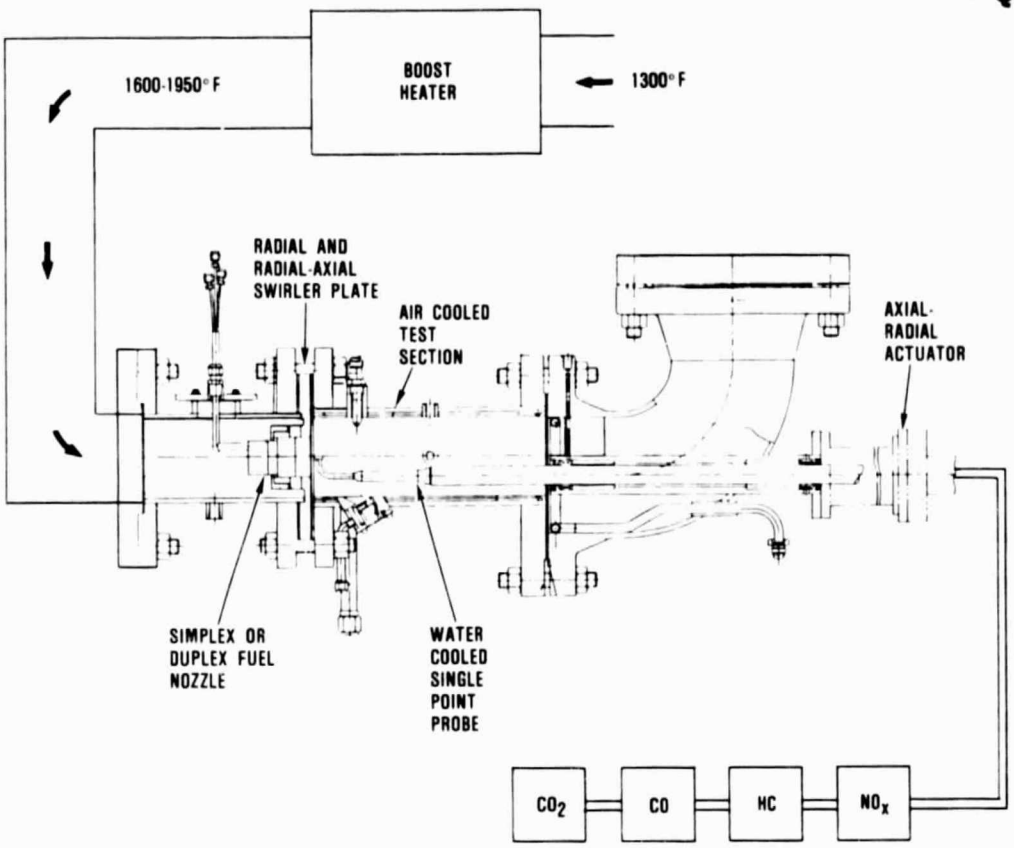

Figure 32. Element Test Rig Setup.

To evaluate a complete engine regenerator system in the static seal leakage rig at Ford, a new cover was designed and fabricated. Due to the greater wall porosity of NGK regenerator material, core leakage across the crossarm and through the inner and outer circumferences is higher when compared with the more dense Corning Glass AS material. Four full-size NGK cores were modified in Japan in an attempt to reduce core leakage. These cores

TABLE 2. SIMPLEX NOZZLE EMISSIONS

	Flat Rated			100% Speed	
Power Setting	Idle	Cruise	Max	Max	Goal*
No_x (g/kg of fuel)	7.93	0.76	1.09	1.29	4.62
CO (g/kg of fuel)	76.53	358.14	17.89	15.45	38.05
HC (g/kg of fuel)	2.34	9.35	0.29	0.27	4.62

*Based on 36.0 mpg urban estimate using DF-2 fuel.

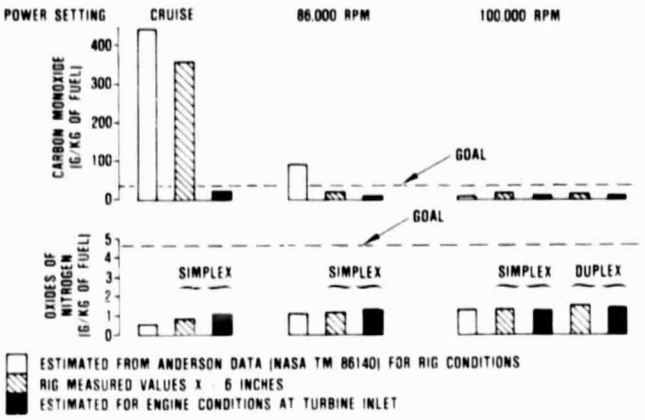

Figure 33. Element Rig Emission Results and Estimated Mod II Engine Emission Levels.

had dense MAS coating applied to the outer and inner peripheries to reduce core porosity leakage. Based on room temperature tests conducted in the static seal leakage rig, core porosity leakage appears to be reduced approximately 50 percent. One core was bonded with a ring gear and sent to Garrett for evaluation in the hot regenerator test rig. NGK also is processing a full size core impregnated with the MAS coating. Static leakage testing of this core will be accomplished upon receipt.

For further reductions in core porosity leakage associated with the NGK cores, a change in material is required. NGK currently is fabricating two full-size AGT cores with the

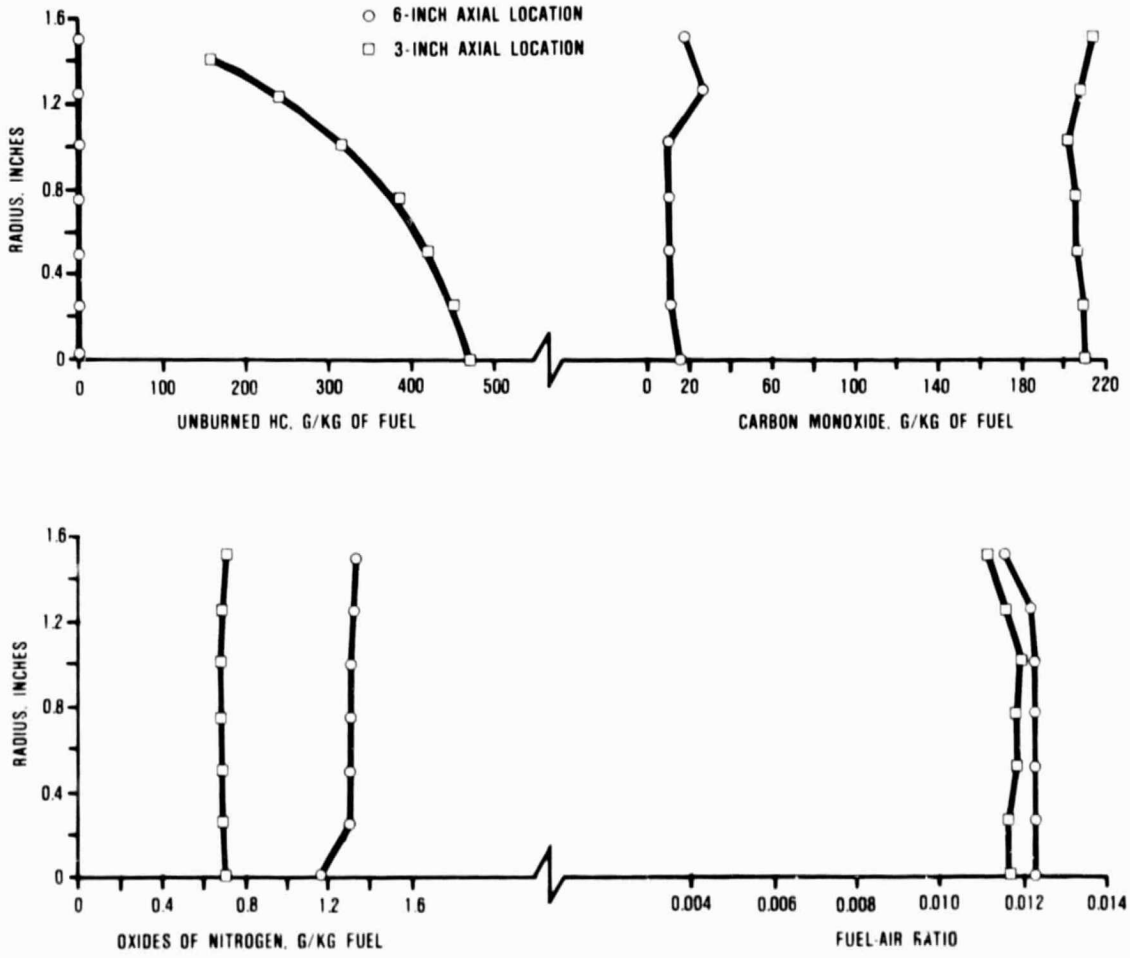

Figure 34. Axial Variation of Species for the Simplex Nozzle (Maximum Power, 100-Percent Speed).

NGK recently developed MAS material (MX). This material has significantly less porosity and higher density, which should reduce porosity leakage to the level of the Corning AS material. Delivery to Ford is scheduled during the early part of the next reporting period.

During this reporting period, NGK developed an extruded rectangular cell opening with an aspect ratio of 1.75 and 0.0043 inch wall thickness. The estimated performance of this cell geometry indicates slightly lower effectiveness (0.5 percent) and considerably greater pressure drop (2.4 percent) at full power when compared to the thin-wall (0.003 inch) isosceles triangular structure cell geometry which meets 1985 performance requirements.

Tests were conducted at Ford to determine the effect of a radial temperature gradient from the inside to outside radius of the circular portion of the outboard seal crossarm. By heating the inside diameter with a pipe-ring resistance heater a radial gradient was imposed uniformly at the center hole region. Outboard seal shoes and complete assemblies have been evaluated with several different end attachments varying from clamped to simple supports. The maximum amount of distortion or coning has consistently been 0.005 inch in the negative direction, which is defined as the coated surface ID being above the OD if the seal were lying face up on a flat surface. Various techniques to relieve the hoop to decrease coning are being investigated.

The primary effort during this period has been to reduce the regenerator seal leakage toward achieving the Mod II objective. The initial two-diaphragm system (Phase I), illustrated on Figure 35, was characterized by marginal seal loading at the part power engine conditions. To apply additional seal loading at the low pressure engine conditions a new three diaphragm system (Figure 35) was designed.

Parametric studies were conducted in the static seal leakage rig to determine the effect of the third diaphragm in the peripheral and crossarm regions. Based on these results the initial three-diaphragm seal system did not significantly reduce leakage when compared with the two-diaphragm system. The third diaphragm was designed to primarily load the

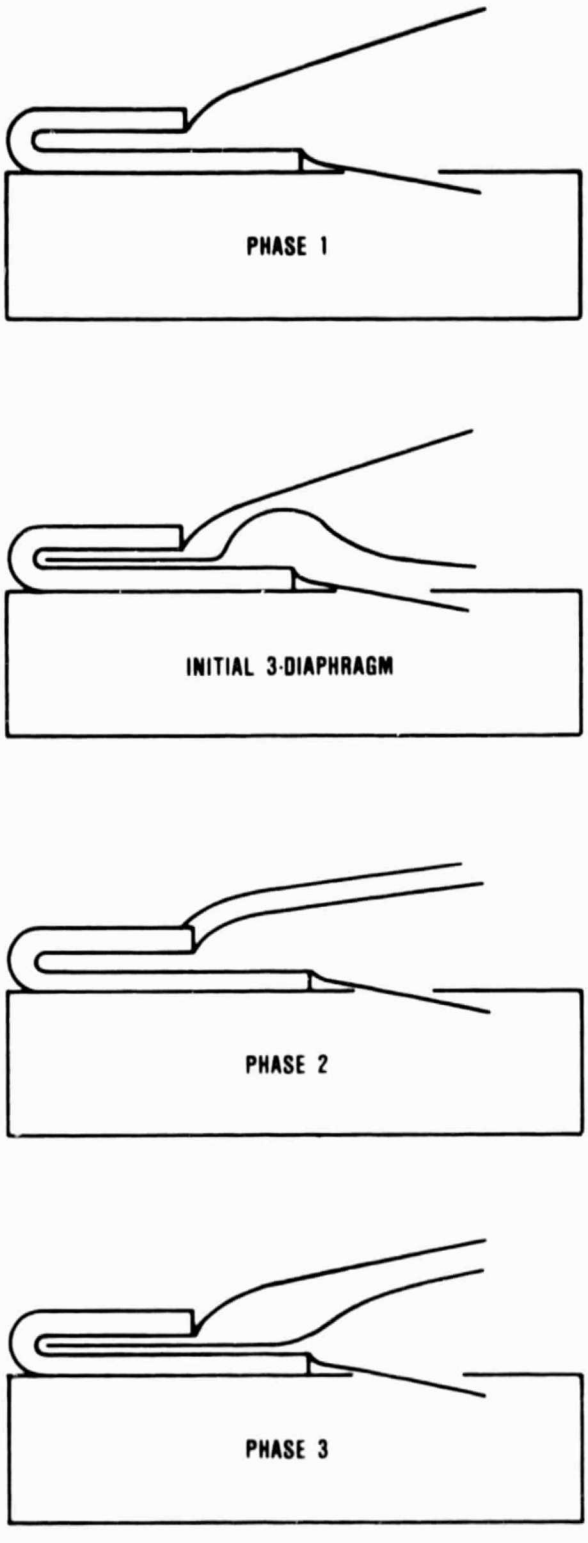

Figure 35. AGT Diaphragm Systems.

upper diaphragm, which is in contact with the engine housing and cover. Investigations in the static seal leakage rig have indicated a need to increase the loading of the lower diaphragm and retainer against the metal substrate. Consequently the third diaphragm was redesigned to accommodate this requirement.

While awaiting dies for the redesigned third diaphragm, a modification was incorporated on the two-diaphragm system on an interim basis. To load the retainer and lower diaphragm to the metal substrate, particularly at part power conditions, an additional diaphragm was spot welded to the outside surface of the retainer (Phase 2 on Figure 35).

Static seal leakage tests conducted both at Ford and Garrett indicate an undesirable leakage sensitivity to diaphragm clearance associated with the Phase 2 seal design. When diaphragm operating clearance is closely controlled, the leakage is significantly reduced when compared with the initial Phase I design, however, sensitivity tolerances are too narrow to be practical in an engine environment.

Based on parametric studies in the static seal leakage rig several design concepts were incorporated into the Phase 3 design, illustrated on Figure 35, to minimize leakage sensitivity with respect to seal "stack" or operating height. Tooling required for the Phase 3 seal design has been completed. Based on test results from the static seal leakage rig, the Phase 3 diaphragm system has significantly reduced leakage with respect to clearance variance. The initial set of Phase 3 seals were sent to Garrett for evaluation in the engine during the next report period.

Analysis of the Phase 3 seal diaphragm system using MENTOR II has been initiated. These diaphragm load characteristics are required for the Core Position Program.

4.5.2 Garrett Regenerator Hot Rig

The hot regenerator rig was assembled with Phase II seals and Corning (Aluminum Silicate) thin walled regenerator core for seal break-in, system leakage, and regenerator performance tests. The recommended total seal working height, based on static leakage tests, was built into the assembled stack.

Testing was initiated for a seal break-in at 1450°F, however, excessive regenerator drive torque was noted ranging from 250 to 300 ft-lbf (torque level for Phase I seals was in the range of 50-100 ft-lbs). An increase in seal working height failed to lower the core drive torque to levels within the rig drive system design limits, and testing was terminated.

Disassembly inspection of the support roller bushings revealed excessive wear on the fixed roller and drive pinion bushings. Subsequent analysis showed contamination of the bushing material as the cause of the high torque problem. The contamination was the result of laboratory duct cooling water leaking into the rig during earlier tests.

4.6 Ceramic Materials and Component Development

Multiple ceramic component deliveries and evaluations were made during this reporting period with the goal of providing hardware suitable for static structures and, ultimately, engine testing. Table 3 summarizes the ceramic components, suppliers, materials and current status. A review of this table indicates that over two engine sets of ceramic hardware (with the exception of the seal rings) are available for evaluation. Additional hardware stock is being prepared. Ceramic components are being provided by six suppliers, often times on a multiple supplier basis.

Of the components listed in Table 3, thermal screening tests of 10 components have been performed in preparation for the planned static structures tests. Screening tests have included multiple, simulated, 1600°F light off cycles performed on 4 turbine shrouds, 2 sets of stators, 2 combustor baffles, and 2 transistion ducts. During these tests, 2 turbine shrouds, later judged to be marginal in quality, were fractured as a result of the thermal conditions. All other components successfully passed a minimum of five 1600°F light off cycles. This testing and the results are discussed further in Paragraph 4.6.1.

Rotor development was highlighted with the multiple spin testing of one ACC bladed rotor to 83,000 rpm and subsequently to 95,400 rpm (95.4 percent of design speed) before

TABLE 3. AGT STATIC COMPONENT DELIVERIES SUMMARY

Component	Source	Material	In-House
Inner Diffuser Housing	ACC	RBSN	2 complete 2 nitrided
Outer Diffuser Housing	ACC	RBSN	2 complete 2 nitrided
Transition Duct	CBO	SASC	6 complete
	ACC	RBSN	1 green
Turbine Shroud	ACC	RBSN	3 machined 1 green 2 nitrided
	CBO	SASC	3 rig quaiity
Seal Rings	ACC/Koppers	RBSN	1 in nitriding
	Pure Carbon	SiC	0
Flow Separator Housing	Corning	LAS	4 engine ready
Regenerator	orning	AS	3, 1 at Ford
	NGK-Locke	MAS	2
Stator	ACC	RBSN	1 set complete 1 set in final grind
	CBO	SASC	1 set
	Ford	RBSN	0
Backshroud	CBO	SASC	6
	NGK-Locke	Si_3N_4	3 engine ready
Regenerator Shield	CBO	SASC	4 engine ready
Combustor Baffle	CBO	SASC	5
	ACC	RBSN	0
Combustor Liner	CBO	SASC	0
		KX02	0
Deswirl Rotors*	ACC	RBSN	3

*Non-engine, rig hardware

fracturing at a surface initiated origin. Results of this testing are presented in Section 4.6.2.

Ceramic interface testing, being performed to assess the compatibility or interaction of the various ceramic material combinations within the AGT101, have identified that several material combinations result in sticking when contact occurs at 1480°F or above. These results have led to an evaluation of coatings as a means of preventing sticking and reducing interface friction. Testing methods and results are presented in Section 4.6.3.

Finally, fabrication development of the RBSN turbine shrouds at ACC has resulted in occasional spalling when these parts are thermally cycled. Several process variables including green density, machining coolant, machining mounting wax and machining technique have been identified as possible contributors to this problem, and a study has been initiated to define those most influential. Meanwhile, process modifications have been incorporated into the shroud fabrication methods to reduce the occurrence of spalling. Two shrouds fabricated using these improved techniques have shown no spalling during initial exposures to 2200°F. This work will be discussed further in Section 4.5.4.

4.6.1 Thermal Screening Tests

4.6.1.1 Description

The thermal screening rigs are designed to subject critically stressed (thermal) hot gas flow path components to simulated engine starting transients to 2100°F. These rigs duplicate engine flow path geometry, thus close approximation of actual heat transfer coefficients is achieved for idle and cruise conditions. This defined operating envelope provides a remote test bed for the testing of individual and/or multiple components in the desired start transient condition. Components are thereby screened on a "Pass/Fail" basis for any given thermal transient.

Further, the rigs add flexibility in the area of component instrumentation (ie, thermocouples attached to the ceramics) such that through wall and flow path thermal gradients can be defined. This information then is fed back into the design loop to confirm and modify (as required) analytical predictions of temperature distribution and temperature induced stresses.

An external combustor provides the heated air supply to the rigs which is monitored with rig inlet and exit thermocouples.

4.6.1.2 Testing and Results

Components tested to date include four turbine shrouds (3 RBSN, 1 SASC), 2 sets of stators (1 RBSN, 1 SASC), 2 combustor baffles (SASC), 2 transition ducts (SASC), and 2 turbine backshrouds (SSN). Testing and results are shown in Table 4.

4.6.1.3 Thermal Screening Tests-- Fracture Analysis

ACC Turbine Shroud S/N 174

A partial reconstruction of this turbine shroud, Figure 36, indicated that fractures initiated at several locations, both at the inner and outer surfaces, in the region of the seal ring land. This region corresponds with the thickest cross-section of the part and, thus, the area most difficult to completely nitride during fabrication. Considerable incidents of material spalling occurred in this region, as shown in Figure 37. These spalling locations were judged the primary fractures from which the secondary and most damaging crack initiation occurred.

A polished cross section of the seal land region of the shroud indicated a large residual area of unreacted Si in the interior of this part, Figure 38. Due to the higher thermal expansion of this unreacted silicon, when compared with the surrounding Si_3N_4 material, stresses that can induce spalling often are generated during heat-up cycles. This spalling activity typically results in sharp edges and irregular surfaces which become sites for secondary crack initiation when thermal stresses during the light off occur.

A component processing history indicated that shroud S/N 174 was cast to a relatively high green density (1.75 g/cm^3) and was ma-

TABLE 4. TESTING AND RESULTS

TURBINE SHROUDS

S/N	Material	Manufactured by	W_A, ppm	Test Temperature, °F	Transient Time, sec	Results
147	RBSN	ACC	10	1800	15	OK
174	RBSN	ACC	10	1600	15	Spalled/fractured
176	RBSN	ACC	10	1600	13	OK
16-3	SASC	CBO	(Scrap-Undersize)	1600	15	Fractured

The shrouds with successful results were each cycled a minimum of 5 times to the stated conditions. S/N 174 spalled during the 1st transient which resulted in complete fracture. (Analysis of the spalling is discussed in Section 4.5.1.3.) S/N 16-3 fractured in an internally delaminated area adjacent to the seal land. This fracture enhanced the role of thermal screening rig as a component proof testing tool. (Fracture analysis is discussed in Section 4.5.1.3.)

TRANSITION DUCT

S/N	Material	Manufactured by	W_A, ppm	Test Temperature, °F	Transient Time, sec	Results
102	SASC	CBO	10	1600	15	OK
103	SASC	CBO	10	1600	15	OK

Both transition ducts tested to date passed without fracture. One will be instrumented for mapping of thermal distribution while the other will be used in the structures rig (S/N 103).

COMBUSTOR BAFFLE

S/N	Material	Manufactured by	W_A, ppm	Test Temperature, °F	Transient Time, sec	Results
102	SASC	CBO	10	1600	15	OK
104	SASC	CBO	10	1600	15	OK

Both combustor baffles tested to date passed without fracture. S/N 104 will be used in the structures rig while the other will be used for mapping.

TABLE 4. TESTING AND RESULTS (Contd)

TURBINE STATORS						
S/N	Material	Manufactured by	W_A, ppm	Test Temperature, °F	Transient Time, sec	Results
Set No. 1	RBSN	ACC	10	1600	15	OK
Set No. 1	SASC	CBO	10	1600	15	Damaged in shroud fracture

The RBSN stator set completed a minimum of five start cycles to 1600°F without fracture or interface deterioration.

During the testing of the SASC stator set the RBSN turbine shroud (S/N 174) fractured due to spalling and 14 of the 19 stators were damaged. It is felt however that the SASC stators would have survived under normal test conditions.

TURBINE BACKSHROUD						
S/N	Material	Manufactured by	W_A, ppm	Test Temperature, °F	Transient Time, sec	Results
103	SSN	NGK	10	1600	15	OK
102	SSN	NGK	10	1600	15	OK

No evidence of material or interface (with turbine stators) degradation was observed. S/N 103 will be used in B/N 1 of the structures rig.

RIG INSTRUMENTATION

The thermal screening rigs utilized acoustic emission probes on the basis of potential early fracture prediction. Background noise thresholds were established for the desired operating conditions and extremely accurate results were obtained during both shroud fracture events. These probes will be used on B/N 1 of the structures rig.

chined in the green condition. Subsequent nitriding resulted in a weight gain of only 58.3 percent (60-percent desirable). Radiogaphy indicated that no detectable defects were present in the finished part. Certification test bars processed in-parallel indicated an average strength and standard deviation of 46.4 and 4.3 ksi, respectively for 12 test bars. These values compare favorably with baseline RBN104 values of 44.9 and 7.8 ksi, respectively, for 30 test bars.*

*All test data generated using four point flexure testing with 1.50 inch outer and 0.75 inch inner spans. Test bar cross sections were 0.250 x 0.125 inches. A cross head speed of 0.02 in/min was used.

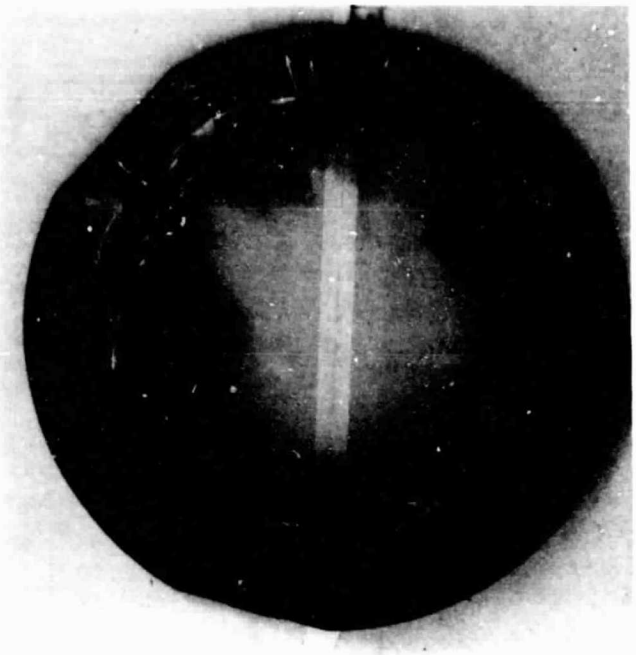

Figure 36. Partially Reconstructed ACC Turbine Shroud, S/N 174 (Arrows Indicate Direction of Crack Propagation).

Figure 37. Spalling Near the Seal Land Region on ACC Turbine Shroud, S/N 174.

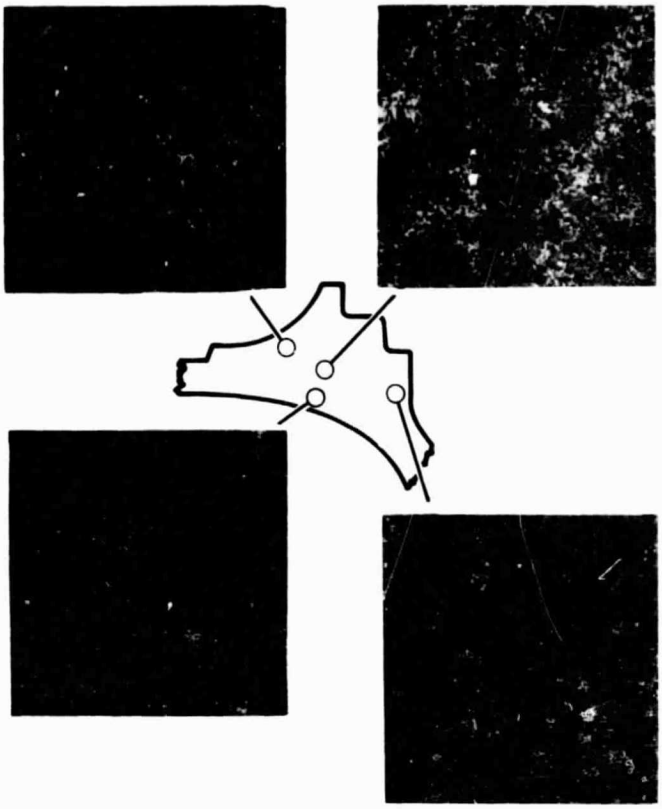

Figure 38. Microstructure of the Seal Land Region of ACC Turbine Shroud, S/N 174.

The processing variables mentioned here are included on a list of potential contributors to the spalling phenomina observed in RBSN material. The study to further identify the significance of these variables is discussed in Section 4.6.4.

Thus, based on the absence of mechanical loading during the thermal screening testing of this part it was concluded that material spalling, followed by thermal stress induced fracture was the turbine shroud failure mode.

Carborundum Turbine Shroud S/N 16-3 Fracture Analysis

Partial reconstruction of CBO shroud S/N 16-3, shown in Figure 39 provided identifica-

Figure 39. Fractured Carborundum Turbine Shroud, S/N 16-3.

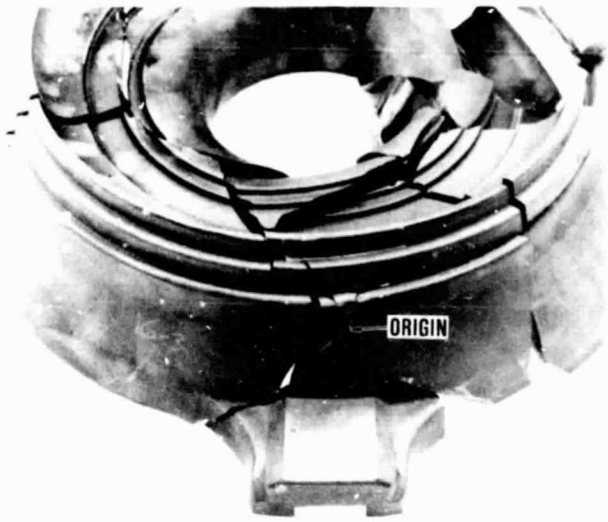

Figure 40. Fracture Origin for Carborundum Turbine Shroud, S/N 16-3.

tion of the fracture origin of the part. Fracture occurred at the analytically predicted peak stress location just forward of the seal ring land region, illustrated in Figure 40. Further examination of this area revealed a planar processing void in the seal land region, illustrated in Figures 41 and 42. As illustrated, this void encompassed approximately one-third of the seal ring region circumference, which would significantly hinder the ability of this component to survive a stressed condition.

X-ray radiography performed by Carborundum on this part failed to identify this process void because radiographs were obtained only in the axial direction (normal to the void plane). However, Carborundum currently is evaluating additional turbine shrouds by obtaining X-ray radiographs taken at several angles around the part.

Figure 41. Processing Void in Carborundum Turbine Shroud, S/N 16-3.

4.6.2 Bladed Rotor Testing

ACC bladed rotor S/N 10191, cast in October 1981, was judged suitable for spin test evaluation based on X-ray radiography, visual inspection and density evaluations. Radiography results indicated no detectable hub defects, but did identify surface bubbles and casting lines in several blades. Visual examination identified additional surface irregularities and several surface cracks in the blade

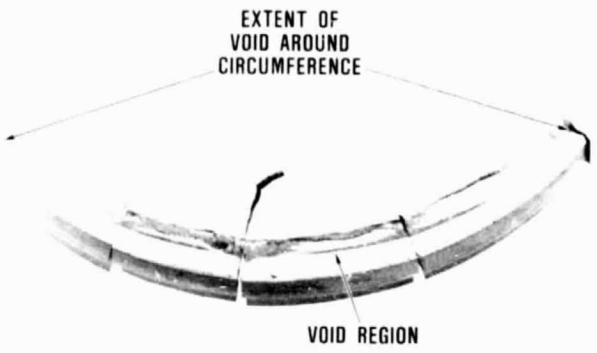

Figure 42. Extent of Void in Carborundum Turbine Shroud, S/N 16-3.

hub interface region. One blade was "tipped" approximately 1/4 inch, which occurred during handling in the as-cast condition. However, the rotor density measurement of 3.09 g/cm^3, compared favorably with the 3.10 g/cm^3 density of the 115,000 rpm successfully spin tested simulated, rotor provided by ACC. Thus, spin test evaluation was performed to verify rotor hub integrity.

Prior to spin testing hand finish and machining operations were performed to minimize visible surface defects. A shrink fit metal shaft was added to the rotor to provide spin arbor attachment. The rotor was balanced using standard multiplane dynamic balancing techniques and material removal.

Initial spin testing resulted in the loss of two blades that entirely fractured within the airfoil sections at 83,000 rpm, as illustrated in Figures 43 through 45. A secondary blade tip fracture occurred in one blade adjacent to one of the two blades; no hub or shaft damage occurred. Visual and 30x microscopic analyses revealed that both blades fractured at surface casting defects.

Rotor rebalancing was achieved by "tipping" blades opposite the fractured two.

The second spin test achieved 95,300 rpm at which time complete rotor destruction occurred. Partial reconstruction of the rotor, illustrated in Figure 46, was possible since

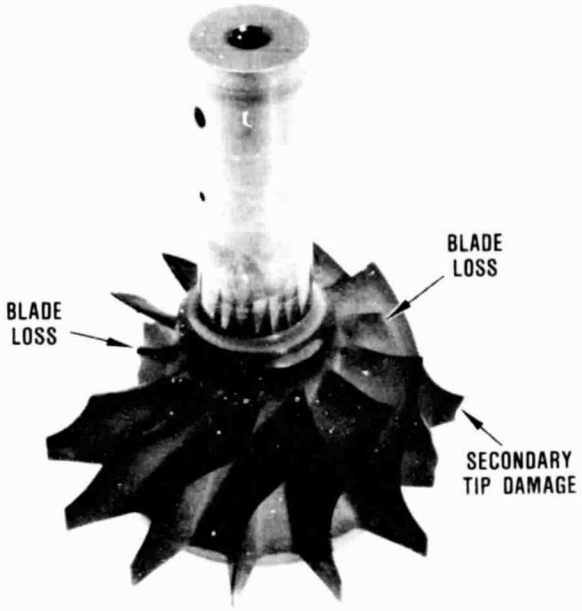

Figure 43. ACC Rotor, S/N 10191, Blade Fractures at 83,000 RPM.

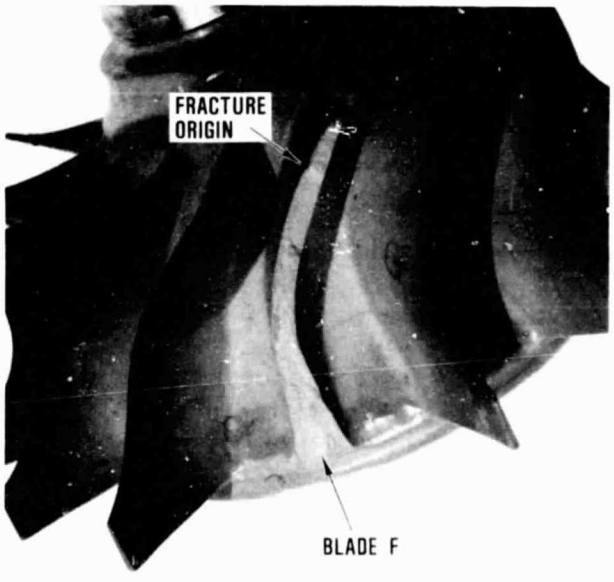

Figure 44. Blade Fracture Origin, Blade F, ACC Rotor, S/N 10191, After 83,000 RPM.

Figure 45. Blade Fracture Origin, Blade M, ACC Rotor, S/N 10191, After 83,000 RPM.

several large pieces of rotor remained. This indicated that although the specific origin is missing, the primary fractures initiated at surface locations as shown in Figure 47. Secondary fractures then propagated inward to the hub. This fracture mode was responsible for the large rotor pieces, not usually observed in hub initiated fractures. Examination of interior fractures revealed no internal defects. One rotor segment was large enough to provide machined subsize test bars. These test bars currently are being evaluated and will be summarized in subsequent reports.

In conclusion, the 95,300 rpm rotor burst results are encouraging from two standpoints. First, the fact that rotor fractures initiated from surface sites, and the lack of observable interior defects confirm the rotor hub integrity. Rotor hub integrity initially was substantiated with the successful spin testing of the bladeless simulated ACC rotor to 115,000 rpm. The current bladed rotor testing indicates the successful transfer of this technology to the

Figure 46. Remains of ACC Rotor, S/N 10191, Partially Reconstructed After Failure at 93,400 RPM.

Figure 47. Surface Fractures on ACC Rotor, S/N 10191.

bladed rotor. Second, the surface features responsible for rotor failure were easily observable prior to spin testing. This fact implies that casting and sintering processes which produce "esthetically pleasing" rotors also will result in improved rpm capability. Processes to improve the visual appearance (ie, surface finish) currently are being applied to rotors being fabricated at Ford and ACC.

4.6.3 Ceramic Interface Compatibility Testing

In conjunction with ceramic component tests, an interface compatibility study currently is being conducted. All interface conditions for the AGT101 have been identified, as shown in Figure 48, along with respective stress and temperature environments for the three engine operating conditions (1600, 2100 and 2500°F TIT). To date, the study has partially evaluated interface conditions I, II, and III for all combinations of material choices. Test bars of as-machined or as-processed material were stacked with a 0.25 x 0.25-inch contract area for condition III. The specimens were heated to the appropriate temperature while dead weight loaded at a minimum simulated engine assembly load. Once at temperature, additional dead weight loads were applied, as required, to simulate engine aerodynamic or mechanical loads and held for 20 hours. Unloading and cool down followed. The

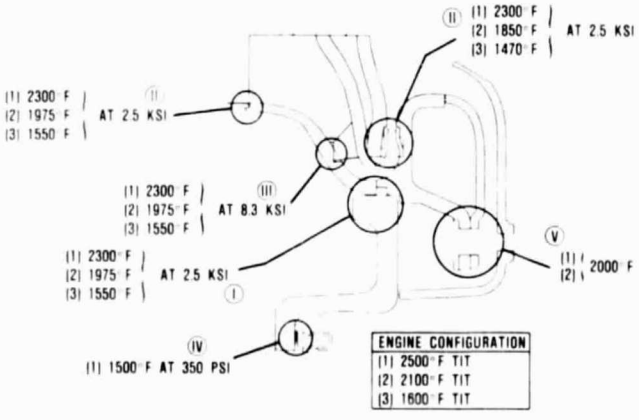

Figure 48. Interface Conditions for 1600, 2100 2500°F TIT Engines.

specimens then were inspected for sticking phenomena. Three classifications were assigned; no stick or reaction (NSR); light sticking (LS) upon cool down, ie, came apart during handling; and hard sticking (HS), not separable by hand. Concern is raised for LS and HS conditions due to the following:

- o LS - longer exposure may result in hard sticking
- o HS - could result in component fracture if the parts thermally expand or cool down at differing rates

Table 5 summarizes the testing for interface conditions I, II, and III. Testing at condition III, depicted in Figure 49, was conducted under a constant 8.3-ksi load (engine assembly preload) and results showed no sticking or reaction.

As noted in Table 5, several material combinations result in sticking under conditions I and II. Additional testing was conducted for these combinations using flame-sprayed mullite coating on one interface surface. Preliminary results indicate that no sticking or reaction occurred with flame-sprayed mullite-coated surfaces.

Although additional testing is planned, and warranted, these preliminary results indicate that the AGT101 ceramic development can pro ceed under the following guidelines:

- o Attention must be given to material combination selection
- o Coated α-SiC or RBSN can be used for selected interface combinations
- o Detailed inspection after test will be conducted to ascertain problem areas
- o Crowned surfaces appear to help in alleviating sticking phenomena

4.6.4 RBSN Spalling Study

Spalling damage has occurred on three ACC RBN 104 turbine shrouds when these

TABLE 5. CERAMIC INTERFACE TEST SUMMARY

Material Combination	Interface[1] I			Interface[1] II			Interface[2] III		
	1470°F	1850°F	2150°F	1550°F	1970°F	2300°F	1550°F	1970°F	2300°F
RBSN/RBSN	-	-	-	NSR	NSR	NSR	NSR	NSR	NSR
RBSN/α-SiC	-	-	-	NSR	NSR	NSR	NSR	NSR	NSR
α-SiC/α-SiC	-	-	-	HS[3]	HS[3]	HS[3]	NSR	NSR	NSR
α-SiC/SiSiC	-	-	-	NSR	NSR	HS[3]	-	-	-
SiSiC/RBSN	-	-	-	NSR	NSR	NSR	-	-	-
RBSN/LAS	NSR	NSR	NSR	-	-	-	-	-	-
LAS/α-SiC	NSR	NSR	HS/CHIP	-	-	-	-	-	-
α-SiC/SN-50	-	-	-	NSR	Dis	NSR	NSR	NSR	NSR
SN-50/RBSN	-	-	-	NSR	Dis	NSR	-	-	-

[1] Evaluated at 0.2, 1.1, and 2.5 ksi

[2] Evaluated at 8.3 ksi, crowned

[3] Mullite coated - NSR

Test Cycle

Heat at 0.2 ksi
Load
Hold 20 Hrs
Unload
Cool at 0.2 ksi

NSR = No stick or reaction

HS = Hard stick

LS = Light stick

Dis = Discolored

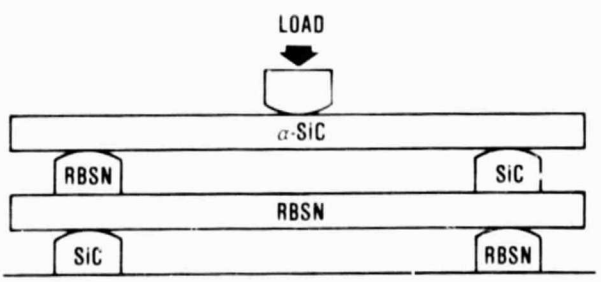

Figure 49. Compatibility Test Condition III Interface Material Combinations.

parts have been exposed to thermal exposure ranging from 1600 to 2200°F. In two instances the spalling resulted in complete destruction of the component, as discussed in Paragraph 4.6.1.3. In the third instance only limited spalling occurred and the turbine shroud subsequently passed 10 simulated lightoff cycles to 1600°F. Spalling of this part currently presents the major obstacle in the qualification of additional hardware.

Spalling typically has been attributed to thermal stress generated within RBSN when

residuals of Si remain un-nitrided during processing. The amount of free Si required to induce spalling has not been quantitifed, however a review of Garrett in-house data suggests that spalling of RBSN parts may occur if weight gains, which occur during the nitriding process are below 59 percent. A weight gain below this figure indicates that a significant portion of Si has not been converted to Si_3N_4 during the reaction process. In addition, high green densities and thick cross sections inhibit free N_2 passage to the interior, which is necessary for complete reaction. Green densities and part thickness limitations must typically be experimentally determined as this fabrication approach is applied to larger or thicker engine components.

Additional influences on complete nitriding include Si purity. Contaminants such as carbon will react with the Si at the elevated nitridation temperatures to form undesirable compositions. Thus, any component processing between green fabrication (ie, casting or molding), may adversely affect the final Si_3N_4 product if contamination may occur.

Current fabrication processing of the ACC turbine shroud requires that green machining occur prior to part nitriding. If mounting compounds and machining coolants are used, the result may be contamination of the porous Si part.

The significance of these and other variables on spalling have been suspect but not methodically studied until now. With the recent shroud spalling occurrences, a joint ACC/Garrett spalling study was initiated. The goal of this study is to identify process parameters most responsible for spalling and to modify turbine shroud fabrication techniques to eliminate the problem. The initial study included the fabrication of several billets of two green densities and thicknesses which have been further processed using various green machining methods. A list of variables for this evaluation is presented in Table 6. After green processing all test plates were nitrided together. Post nitriding machining will be performed on several billets then thermal cycling will be performed. All billets currently are in final machining.

TABLE 6. RBSN SPALLING STUDY VARIABLES

Green Process Variables	
Green Density:	Low vs high
Machining Variables:	Machined vs no machining
Machining Mounted:	Mounting compound versus no mounting compound
Machining Coolant:	No coolant vs coolant
Machining method:	Milling vs grinding
Final processing variables	Machined vs as-nitrided

Meanwhile, turbine shroud fabrication techniques also have been modified to reduce the spalling occurrence. Parts now being fabricated have a lower green density and are green machined with no coolant and minimal mounting compound. Mounting compounds are subsequently machined off the Si surfaces prior to the final cleaning operation to prevent compound penetration into the green part. Although results are not complete, two turbine shrouds processed using these methods were thermally cycled to 2200°F after nitriding with out any occurrance of spalling.

Studies will continue and will be reported on in subsequent reports.

4.7 Foil Gas Bearing

Phase II testing will evaluate high temperature foil bearings (Figure 50). The high-temperature foils will be coated with Titanium carbide and the turbine journal will be coated with SCA (Silicon, Chromia, Alumina). All high-temperature test rig hardware has been received, and Phase II testing will immediately commence.

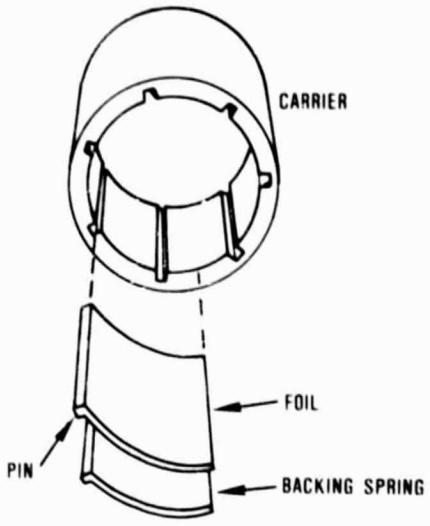

BASIC BEARING CONFIGURATION

NUMBER OF FOILS AND SPRINGS	7
THICKNESS OF FOILS	0.006 INCH
FOIL ARC LENGTH	1.190 INCHES
FOIL AXIAL LENGTH	1.075 INCHES
FOIL PREFORMED RADIUS	0.850 INCH
SPRING "X" DIMENSION AND AXIAL LENGTH	0.005 x 0.585 INCH
SPRING PREFORMED RADIUS	0.700 INCH
SWAY SPACE	0.010 INCH
COATING TEFLON S	0.001 INCH THICK

Figure 50. Foil Bearing Geometry.

4.8 Rotor Dynamics Development

Investigation of the high-temperature foil bearing was initiated, utilizing the high-temperature test rig shown in Figure 51. Stability problems with the rig drive motor delayed checkout and testing of the high-temperature foil bearing rotor dynamics.

Concurrent with procurement of the rig hardware, the turbine wheel was SCA-coated and the foils for the high-temperature foil bearing test were coated with Titanium Carbide (TiC). The hot rig rotating assembly was balanced and readied for installation. The heater control and instrumentation were assembled, checked out and installed for the high-temperature foil bearing tests.

Figure 51. Foil Bearing Test Rig Assembly.

The axial thrust load on the high temperature rig is provided by a magnetic load on the rotating assembly. Preliminary tests were done to evaluate the load capability of the magnet.

4.9 AGT Controls and Accessories

Installation and initial engine test operation of the full authority digital electronic control unit (ECU) was accomplished during January 1982. The addition of the ECU to the control system provided automated start sequencing, closed loop speed and temperature control, and the added primary protective features for overtemperature, underspeed, overspeed, low oil pressure, high oil temperature, and flameout.

Minor problems with speed signal conditioning, electrical harness pin assignments, and pressure transducer calibration were resolved prior to and during the first few engine test runs. The speed conditioning circuitry in the ECU initially was incompatible with the signal quality of the engine integral Bentley speed sensors. Temporary modification of the ECU allowed operation of the control system utilizing a laboratory monopole until problems of Bentley sensor installation (on subsequent engine builds) and revisions to the speed conditioning circuits were implemented.

This preliminary phase of control system checkout and evaluation also included several refinements and adjustments to the control software, which included a closed loop T4 (turbine inlet temperature) start schedule in place of T5 (turbine exit temperature), T4 overtemperature limits in place of the existing T5, and other minor schedule, logic, and limit changes. LBO (lean blow out) limits in the fuel schedule also were reduced to only 20 percent of the original value, due to the exceptionally good LBO characteristics of the combustor. All of these logic changes were readily accomplished through relatively simple "patches" to the control software.

Engine testing resumed in April 1982 using the same controls hardware and software that existed when engine testing ended in January 1982. After preliminary engine checkout runs were completed, a new substantially enhanced software configuration was installed and ran successfully without incident.

Hardware modifications subsequently added to the ECU included speed circuit changes (mentioned above), and conversion from a proportional fuel torque motor control signal to PWM (pulse width modulated). Bench test results for the PWM fuel control have been demonstrated in the laboratory to substantially reduce hysteresis, as evidenced by fuel flow versus torque motor current data. Assembly and extensive testing of the PWM configuration fuel control hardware was completed prior to installation and checkout on the engine.

APPENDIX A

FORD MOTOR COMPANY
ADVANCED GAS TURBINE (AGT) POWERTRAIN SYSTEM DEVELOPMENT PROGRAM
FIFTH AGT SEMIANNUAL TECHNICAL PROGRESS REPORT

1. Task 2.3 - Ceramic Rotor

1.1 Material Development and Characterization

The properties of Ford RM-2 sintered reaction bonded Si_3N_4 rotor material were presented in Reference 4. As reported, an anomaly in the oxidation kinetics was noted at 1832°F (ie, the oxidation was more severe at this temperature than at both higher and lower temperatures). However, this appeared to have only a minor effect on strength after static oxidation exposures up to 700 hours.

During this reporting period, four-point bend stress rupture tests were performed at temperatures from 1832 to 2192°F at stress levels of 20 to 90 ksi. For temperatures above 2051°F, no time dependent failures were observed for test times exceeding 600 hours. These results were independent of stress level.

However, time dependent failures were observed at 1832°F and low stress levels (20 ksi). Ten tests were performed at these conditions, with failure times ranging from 19-93 hours. The characteristic failure life was 56 hours with a Weibull slope of 2.4; the Weibull plot of these ten test results is shown in Figure 52.

It was determined that the 1832°F oxidation could be reduced by use of a "Flash oxidation" process, which consists of a rapid heating to a high temperature followed by a short hold time at temperature. An air atmosphere is employed. This process forms a thin oxide surface layer that reduces oxygen diffusion into the base material. Oxidation kinetics of these treated materials were shown to be stable out to 300 hours at 1832°F. The level of oxidation also is dramatically lowered. Figure 53 is a typical plot showing the oxidation kinetics at 1832°F.

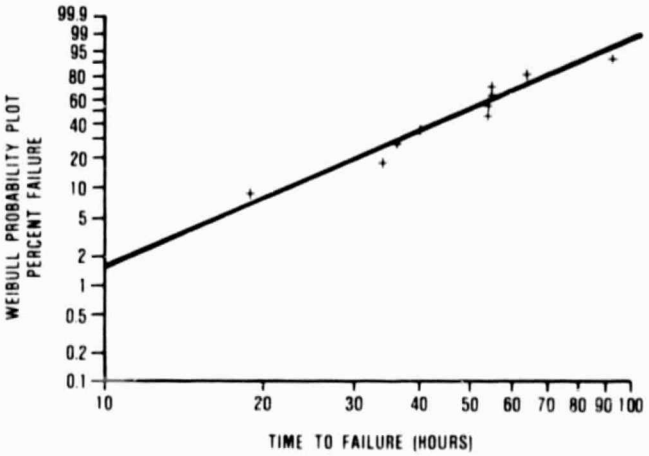

Figure 52. Results of Stress Rupture Tests of RM-2 at 1832°F and 20 ksi Load.

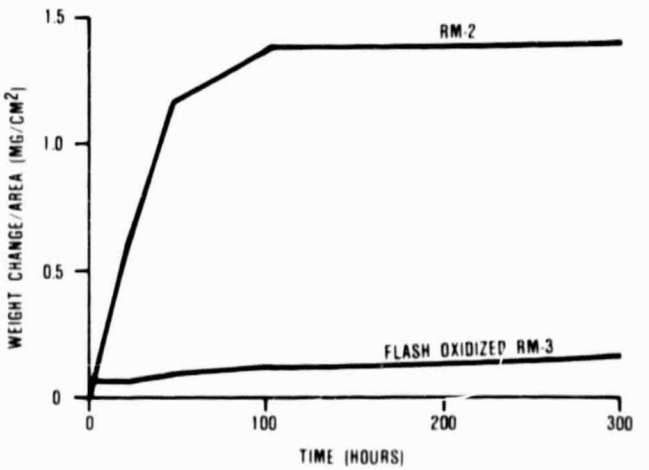

Figure 53. Oxidation Kinetics at 1832°F of RM-2 and "Flash Oxidized" RM-3.

Preoxidized RM-2 material has been given the designation of RM-3. Stress-rupture tests for RM-3 material at 1832°F and 40 ksi load show no time dependent failures out to 500 hours. The "flash oxidation" conditions are being optimized with respect to the stress rupture properties of the material. Once these conditions are finalized, a complete characterization of RM-3 properties will be performed.

1.2 Bladed Rotor Fabrication

Efforts continued to improve the slip casting process for forming of bladed rotors. While rotors were cast that visually looked good, detailed microscopic inspection of rotors in the nitrided state (the first opportunity for close examination) revealed tight cracks of varying lengths in the hub, blade root, and shaft regions. In addition, nitrided bulk density variations exceeded the target density window of 2.3-2.4 g/cm^3. Material with density below 2.3 g/cm^3 would not sinter to full density, while material with density above 2.4 g/cm^3 would not nitride completely due to the thick hub section.

To understand and solve these problems, a more basic approach was taken to relate slip properties to casting behavior. The rheology and chemistry (expressed by pH and hydrogen evolution) of the Si + Y_2O_3 + H_2O casting slips were unstable with respect to time. Attempts to alter this behavior by altering the ionic nature of the slip, through changes in pH or by altering the deflocculant type and concentration level generally were unsuccessful. However, one deflocculant was found that would stabilize the rheology, but not the chemistry. The pH was observed to change as a function of time. Hydrogen also continued to be evolved from the slip as a function of time.

The green density and casting rates were found to be a function of the slip rheology. Generally, the slip rheology could be expressed using the Casson equation $\tau^{1/2} = \tau_y{}^{1/2} + C^{1/2}\dot{\gamma}^{1/2}$ where τ is the shear stress of the slip, $\dot{\gamma}$ is the shear rate and $\tau_y{}^{1/2}$ and $C^{1/2}$ are constants. τ_y corresponds to the yield stress of the slip while C corresponds to the infinite shear rate velocity of the slip. The constant τ_y was the parameter most useful in characterizing slip behavior. Figure 54 shows how τ_y varies as a function of slip rheology. Figure 55 shows qualitatively the relation between τ_y and casting properties. From these relations the slip rheology could be defined that offered the opportunity for obtaining the correct green density and casting time.

The physically stable slips that have been produced are dilatant ($-\tau_y{}^{1/2}$) and fall outside the desired slip rheological specification.

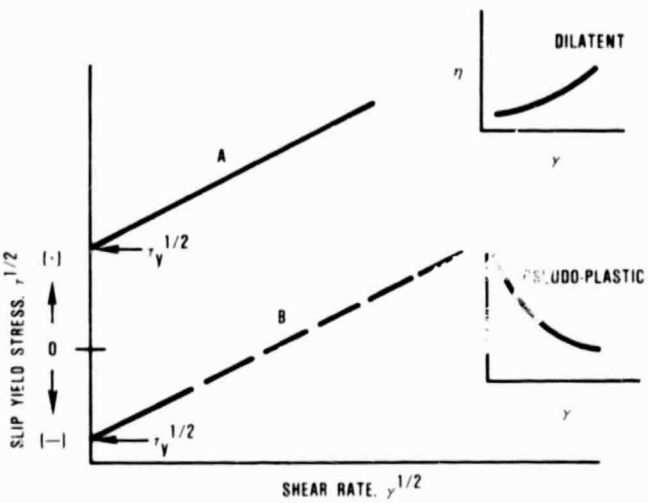

Figure 54. Qualitative Representation of Two Casting Slips; A Being Dilatant ($-\tau_y{}^{1/2}$) and B Being Pseudo Plastic ($+\tau_y{}^{1/2}$).

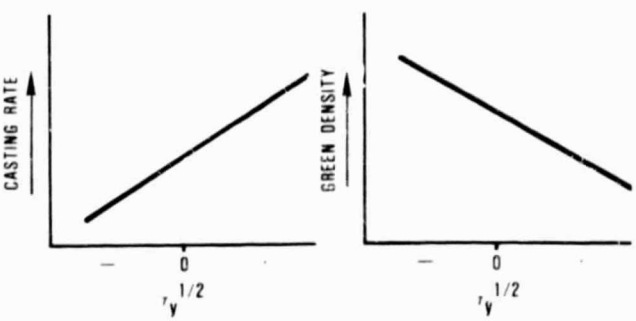

Figure 55. Qualitative Representation Showing the Relation of Slip Yield Stress ($\tau_y{}^{1/2}$) to Casting Rate and Green Density of the Part.

Casting rates of <1.2 cm/hr and resultant green densities of 1.7 g/cm^3 (2.6 g/cm^3 nitrided density) were observed with these dilatant slips.

Attempts were made to alter the rheology to pseudo plastic ($+\tau_y^{1/2}$), which is required to obtain the desired casting rates of ≈3 cm/hr and green densities of ≈1.5 g/cm^3. While this has proven to be difficult, results late in the reporting period confirmed that pseudo plastic slips that produced rotors of much i proved quality could be made within the desi:ed casting time and near the desired green density.

Based on these results, future work will concentrate in the chemical and rheological control of the slips.

2. Task 2.7 - Stator-Ford

Molding development continued using 2.7 g/cm^3 density RBSN material. Parametric investigations into the effect of cavity pressure on compo:ent quality identified three problems:

- o Severe parting line flash occurred at molding pressures above 5000 psi, well below the design molding pressure level of 7500 psi
- o Stator shroud axial thickness varied with injection pressure significantly more than expected
- o A nonsymmetric fill pattern was occurring through the circumferential gate

The severe flash was a result of insufficient die/platen rigidity. After confirming that the full clamping load was being applied, measurements of platen and die deflections during high pressure molding indicated that the tool was inadequately supported in the center section. By shimming the tool/platen interfaces to concentrate the full clamp load through the central section of the tool, molding at full cavity pressure could be done without flash.

Measurements of shroud thickness continued to show an increase with injection pressure. Also, after redirecting the clamp load path, the ejector pin depressions in the molded part increased in depth. Both of th:se occurrences were traced to internal deflections of tool parts. Spacers were added without reworking the tool, reducing the dimensional variations and the pin depressions to levels acceptable for continued parametric studies.

A series of short shots was made to investigate the fill pattern. This study indicated that a non-uniform fill pattern developed after the material reached the circumferential gate. Trailing edge knit lines also were observed, predominately in the area that began to fill first. Gate width measurements on molded parts indicated that a gate eccentricity amounted to a 40-percent variation in gate size from side to side. The tool was reworked in-house to form a slightly larger, concentric gate and uniform fill patterns were obtained. Trailing edge knit lines were still being observed, however, molding parameters were identified such that the knit lines have no depth in the molded state.

A broken tool insert required removal of the tool for repair at the supplier. Analysis of the insert failure identified the cause as hydrogen embrittlement, which was traced to the omission of a post-plating heat treatment. While a replacement insert was being fabricated, several additional permanent modifications were incorporated to internally stiffen the tool.

Since several additional inserts were found to have embrittlement cracks, a complete set of new inserts has been ordered. The new set also will include design changes authorized by Garrett to increase the vane trailing edge thickness from 0.030 to 0.040 inch in an effort to further reduce trailing edge knit lines. The repaired tool has been returned from the supplier for continued molding development while the new inserts are being prepared.

Several stator segments and complete stators have been burned out and nitrided. A nitrided stator, shown in Figure 56, has been dimensionally checked for machinability and to confirm the shrinkage rate used in tool design.

2.1 Task 2.7 - Flow Separator Housing-Ford

No work was planned or carried out on this task during the reporting period.

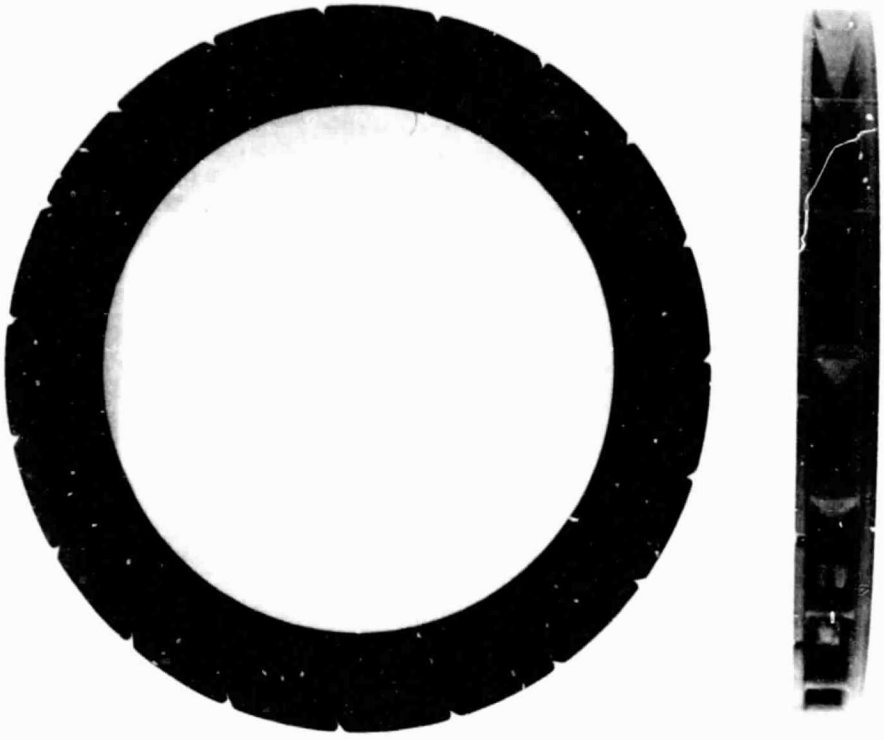

Figure 56. Nitrided Monolithic Injection Molded Stator.

APPENDIX B

AIRESEARCH CASTING COMPANY (ACC)
ADVANCED GAS TURBINE (AGT) POWERTRAIN SYSTEM DEVELOPMENT PROGRAM
FIFTH AGT SEMIANNUAL TECHNICAL
PROGRESS REPORT

1. SUMMARY

Fabrication of SNN bladed rotors using patterns containing the 14.5 percent shrinkage allowance continued. Several process and material parameters were evaluated. These include variations in drying time, temperature and humidity control; powder preparation procedure (calcining and remilling); sintering variations (time, temperature, heating rate and component location in furnace); slip additives; and kiln furniture history. Tooling for bladeless rotors for dynamic spin test evaluations has been fabricated and six rotors have been cast.

Ceramic structures have been processed and shipped. This includes several configurations new to this report period such as combustor baffle, turbine transition duct, deswirl rotor and seal rings.

Improved density control and machining techniques have led to components with higher weight gains and reduced tendency to spall in oxidation treatment cycles.

2. ROTOR - MATERIALS AND FABRICATION DEVELOPMENT

2.1 Fabrication Development

During this report period, SNN rotors were cast in molds containing the 14.5 percent shrinkage allowance. Two fabrication techniques were evaluated. One with the backface (dome) down in plaster and the second, with the backface up (inverted). The dome down position resulted in reduced casting time and improved appearance. This method was adopted for subsequent rotor castings. Figure 57 illustrates the dome down in plaster technique.

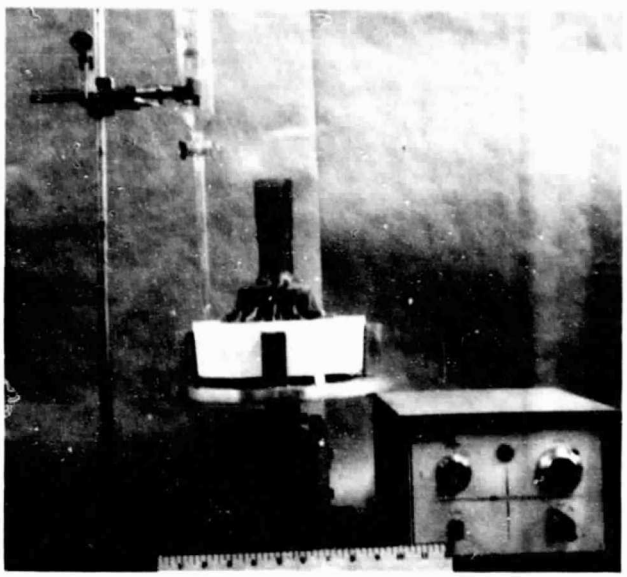

Figure 57. Dome Down in Plaster Technique for Slip Casting of Sintered Si_3N_4 Bladed Rotors.

The organic shell molds were produced by dipping the reusable rubber rotor pattern into an advanced shell mold material. The mold thickness is increased by continued dipping into a molten batch of water soluble wax. The pattern then is extracted from the mold and the water solubie wax is dissolved away. Figure 58 shows the successive steps.

Variations in drying time, temperature and humidity were evaluated. The microprocessor controlled humidity oven has been installed, (Figure 59); requiring several time consuming dry runs to establish control parameters. Work is satisfactorily progressing and will permit accurate control of optimized drying cycle environment for establishing production drying

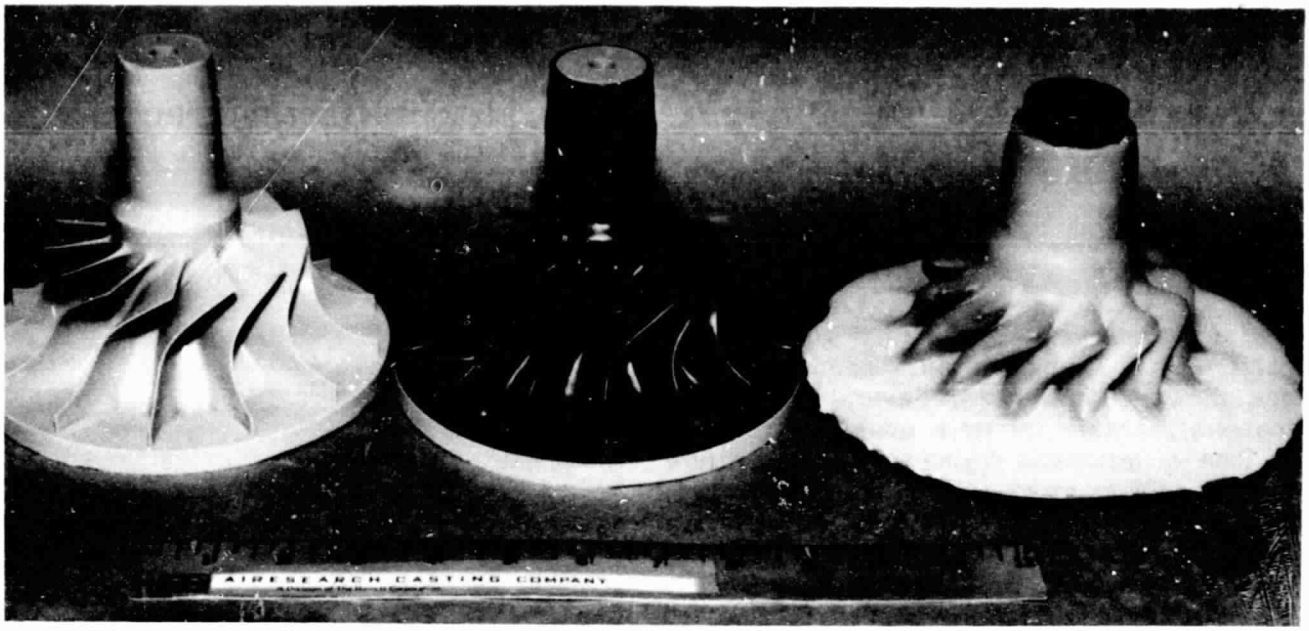

Figure 58. Pattern, on Left; After Dipping in Mold Wax, Center; Reinforced with Water Soluble Wax and Pattern Extracted on Right.

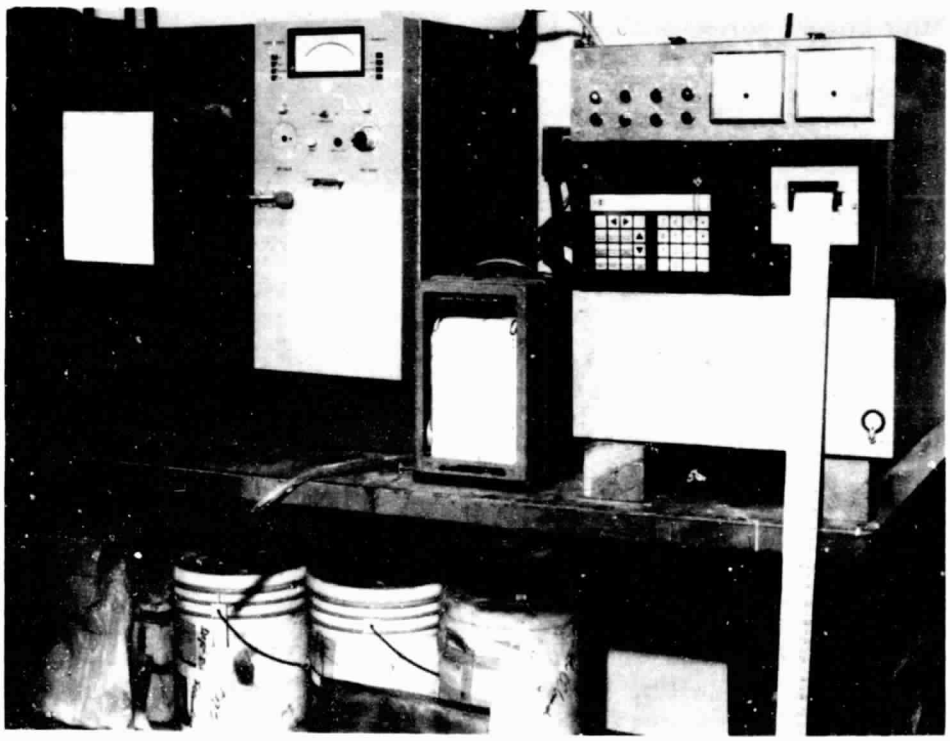

Figure 59. Micro-Processor Controlled Humidity Oven.

cycles and to accelerate the development effort. Although a backlog of rotors awaited sintering, the actual sintering was delayed pending process variation evaluations to provide reproducible, high density castings.

Casting behavior, material uniformity, batch reproducibility, final density and strength are the principle criteria for evaluation of process changes. Process variations studied were the powder preparation procedure (calcining and remilling) and selected sintering parameters.

An initial powder preparation experiment was completed. Table 7 shows the plan by which variations were studied. Table 8 shows the results summarized to show the effects of the variables. Slip viscosity indicates the ease of slip handling and mold fill, low values being more fluid. All variables showed significant influence on viscosity; especially milling time. Gelation refers to losing flow capability prior

TABLE 7. POWDER PREPARATION VARIABLES

Slip No.	Temp., °C	Mill Time, hours	Mill Type	Presinter Cycle
1	1100	6	Wet	Y/N(1)
2	1200	6	Wet	Y/N
3	1100	24	Dry	Y/N
4	1200	24	Dry	Y/N
5	1100	6	Dry	Y/N
6	1200	6	Dry	Y/N

(1) Y/N, yes/no, all process combinations were evaluated with some samples fired to 2150°F prior to sintering and some samples sintered as-cast.

TABLE 8. POWDER PREPARATION RESULTS

Condition	Slip Viscosity, cps	Gelation	Casting Rate (1)	Sintered Density, g/cm^3
1100°C	70	None	11.2	3.14
1200°C	90	None	9.1	3.10
6 hours (dry)	110	None	10.5	3.12
24 hours (dry)	52	None	9.0	3.12
Wet (6 hours)	72	Some	12.0	3.10
Dry (6 hours)	110	None	9.8	3.12
As-cast	(2)	(2)	(2)	3.15
Presintered	(2)	(2)	(2)	3.08

(1) Relative casting thickness in 1/16-inch increments for 3-hour casting

(2) Does not apply

to becoming a dense casting. Gelation occurred only where wet milling was performed and is probably an indication of over milling. Casting rate also is affected by these variables. Potentially, the higher casting rate will provide greater uniformity within a casting.

Sintered density is strongly affected by the powder calcining temperature.

Reduced calcining temperatures revealed improved material uniformity as shown by fracture surface studies. Calcining is conducted to improve the stability of Y_2O_3 in water based slips. Improvements in Y_2O_3 processing resulted in a powder more stable in water leading to greater slip stability. Further improvement could lead to the ultimate elimination of the calcining step in the process.

To verify the results and provide additional data, a similar experiment was initiated with the following conditions: 1832 versus 2012°F, six versus twelve hours, and presintering versus no presintering. Sintering parameters also were evaluated. Variable results to date have been attributed to controlled variation of peak temperature, heating rate, and furnace load arrangement. Test bars were prepared (by injection molding for simplicity) and sintered with the following conditions: 3182 versus 3272°F, low versus high furnace position, sealed versus vented furnace liner, and slow versus fast approach to final temperature. Variations in sintering soak temperature, cycle rates and furnace load arrangement revealed a strong correlation between low weight loss and high strengths. Strengths up to 104 ksi were measured with density varying from 2.86 to 3.16 g/cm^3. Presintering did not appear to be significant in controlled test conditions.

The casting evaluations resulted in rotors that are void and crack free and are potential spin test candidates. Figure 60 shows the excellent blade detail of one such casting. More complete results of sintering evaluations are yet to be obtained.

Distortion of components has been caused by temperature gradients within the chamber. Air leakage also was identified. These have been corrected.

Figure 60. As-Cast Rotor Showing Excellent Blade Detail.

Kiln furniture history has been shown to be far more significant with respect to the sintering behavior of the ware than was originally thought. Furniture that had originally been used in oxidizing atmosphere cycles had a detrimental effect on sintering. Consequently, new kiln furniture has been fabricated for exclusive use in sintering of components.

A pattern was received from Garrett for a bladeless rotor for dynamic spin test evaluation. Six have been cast. The configuration of as-cast rotors can be seen in Figure 61.

Five sintered shafts for shaft attachment studies have been shipped to Garrett for evaluation.

2.2 Material Development

Experiments were conducted to evaluate various slip additives such as dispersants and defoaming agents. A new dispersant has been

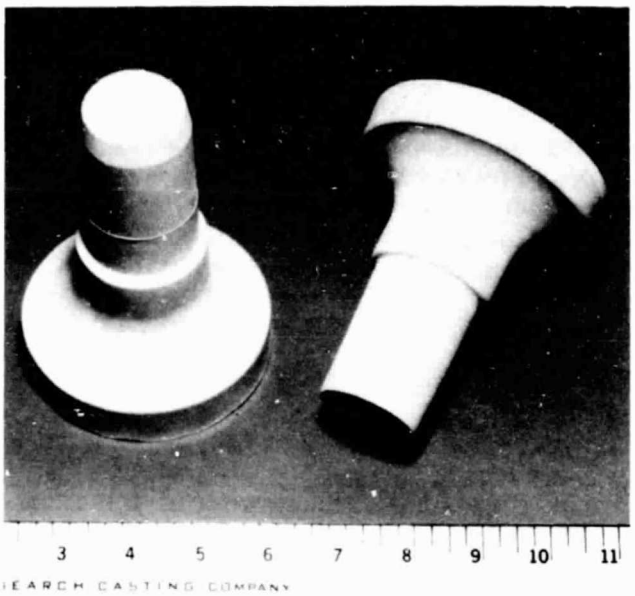

Figure 61. Bladeless Rotors for Dynamic Spin Test Evaluation.

identified, which appears to produce useful slips from powders originally thought to be not readily castable, as well as to show improvement in present slip systems.

Discussions were held with technical representatives of suppliers of commercial defoaming agents who have recommended several products. Samples are being supplied by W. R. Grace, and Rohm and Haas, companies. It is expected that an effective defoaming agent will eliminate voids in castings caused by entrapped air bubbles.

3. CERAMIC STRUCTURES

3.1 Turbine Stator

Injection molding of 40 RBSN visually (30x) and x-ray acceptable stators was completed. It was decided to conduct binder removal on small groups to enhance the probability of supplying a complete engine set. Fourteen have been nitrided and shipped to Garrett. The remaining 26 are ready to be nitrided. During this period parametric studies, which included the use of alternate binder systems, were initiated in an effort to improve injection molding quality. One such experimental binder is a plastic based system which provides excellent bond strengths. Alternate removal cycles also are being evaluated. Figure 62 shows an individual as-injected stator vane and a partially assembled stator ring. Figure 63 shows a complete ring.

3.2 Turbine Shroud

Six nitrided shrouds were shipped to Garrett for final grinding and evaluation. S/N 147 had a uniform thickness outer flange whereas the remaining five contained the bolt attachment lugs in compliance with the latest

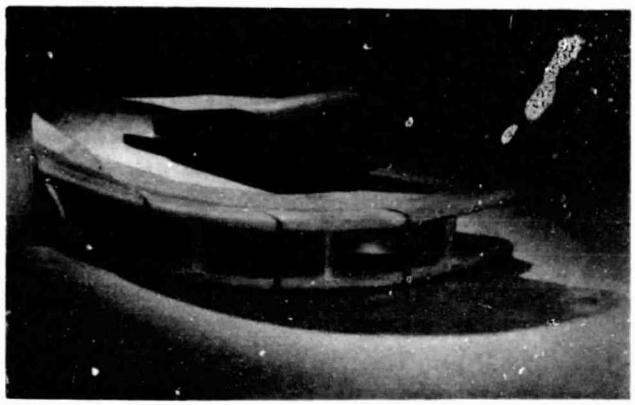

Figure 62. As-Injected Stator Vane and Partially Assembled Stator Ring.

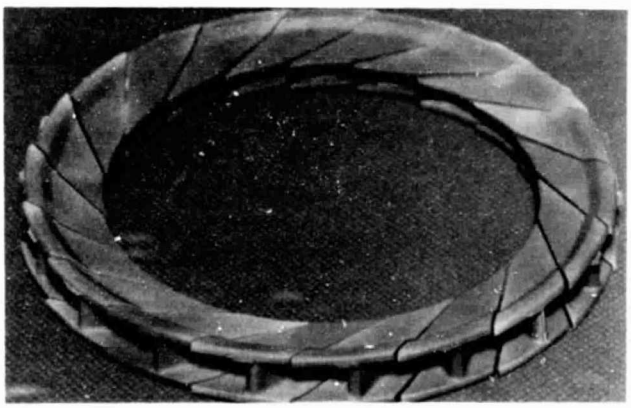

Figure 63. Fully Assembled RBN-124 Stator Ring.

design change. One shroud, S/N 150, was returned for 2200°F oxidation and spalled in that cycle. To verify that this phenomenon was not an inherent material problem, three shrouds, nitrided in the as-cast condition, were subjected to 1600 and 2200°F oxidation cycles. No spalling occurred in these samples. To identify the source of spalling, thick plates were cast from which variables such as density, thickness, machining techniques, stock removal after nitriding, and deliberate contamination are being evaluated. Four shrouds were cast at and below normal density (1.70 - 1.72 g/cm^3) and were shipped to Garrett for green machining and evaluation. Two of these have been returned and nitrided and both measured higher than usual weight gains (60.7 percent). The higher weight gain is attributed to improved machining techniques, reduced cross section thickness and low casting density. These can be seen in Figure 64.

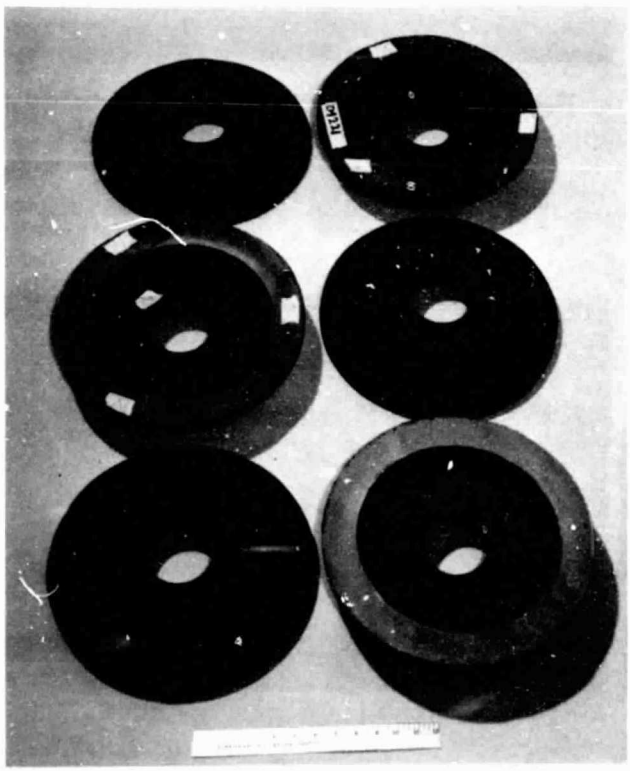

Figure 64. AGT101 Turbine Shrouds.

Density control has been accomplished in slip cast structures by casting density samples prior to the actual casting of components. Immersion density procedures are used employing an organic solvent instead of water. Errors in measurement resulting from temperature induced solvent density variations have been identified. Consequently, corrections now can be made to permit accurate density control.

3.3 Turbine Inner Diffuser

Four inner diffusers were cast and all cracked during the early drying stages. This cracking was attributed to wear of the multipiece plaster molds. This mold wear (due to normal use) resulted in some rough edges at the mold parting lines and, possibly, slightly rougher surfaces on the plaster finish. Both wear effects result in castings that do not easily release from the molds, and the rough mold edges may result in irregular surfaces or stress risers in the casting. The combination of these influences can contribute to cracking during the initial part shrinkage, or during part removal from the mold. New molds have been fabricated for use in future castings to avoid these problems.

One machined and nitrided inner diffuser was received from Garrett for 1600°F oxidation treatment. This was completed with no evidence of spalling and was returned to Garrett.

3.4 Turbine Outer Diffuser

Two nitrided and final machined outer diffusers were received for oxidation treatment. No spalling occurred and the components were returned to Garrett. Two additional outer diffusers, S/Ns 182 and 183, were nitrided and shipped to Garrett for final grinding. One more outer diffuser, casting number 1215101 and an associated certification plate were prenitrided. Test bars were machined from the plate and will be nitrided with the outer diffuser. Examples of both inner and outer diffusers are shown in Figure 65.

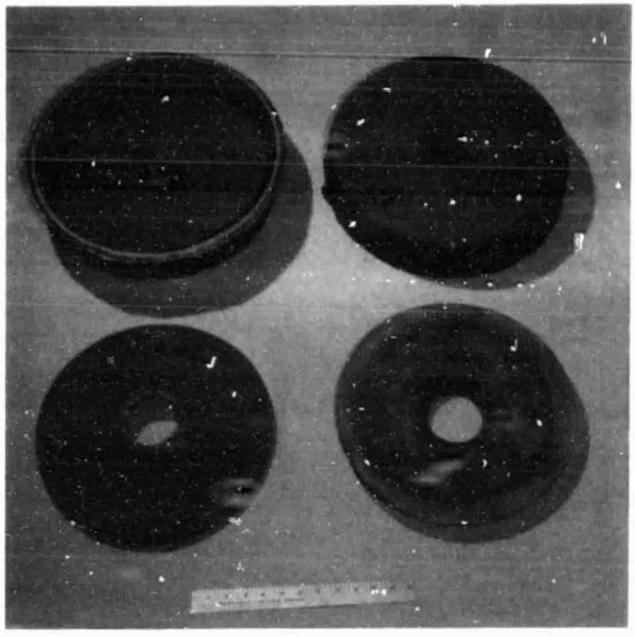

Figure 65. AGT101 Inner (Top) and Outer (Bottom) Diffusers.

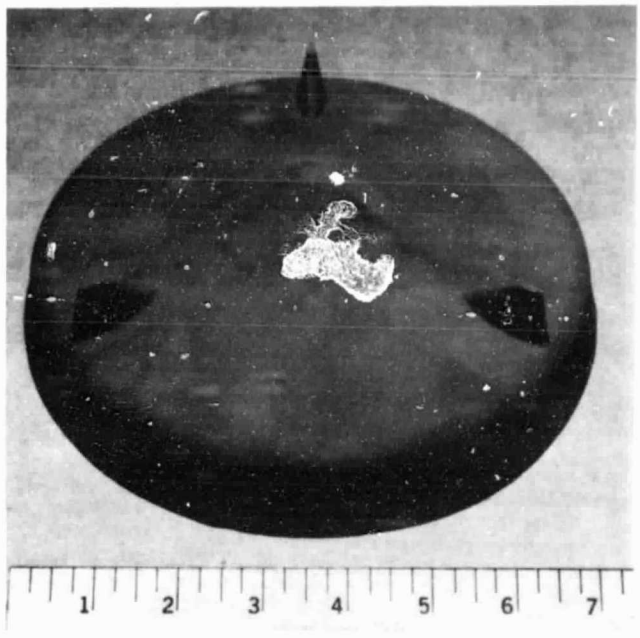

Figure 66. AGT101 As-Cast Turbine Baffle.

3.5 Turbine Baffle

Tooling was ordered and delivered on schedule. Trial castings demonstrated the ability to cast the baffle with integral lugs.

One piece was cast and prenitrided (Figure 66). Following machining of certification bars, this casting will be nitrided as-cast. Additional castings were prepared which are suitable for green machining process development at ACC.

3.6 Combustor Transition Liner

An order for tooling was placed and delivered on schedule. Molds were prepared and trial castings indicated no casting difficulties. One part, S/N 210, was shipped to Garrett for green machining.

3.7 Deswirl Rotor

A metal sample was provided to ACC by Garrett. The sample was readily adapted for ACC mold fabrication. Five pieces were cast to establish a procedure for test hardware.

Six deswirl rotors were cast. Densities were held low (1.66 - 1.72 g/cm^3) in view of the need to nitride the thick cross section. A series of 0.188-inch diameter holes have been drilled in the low stress hub to enhance nitriding.

Castings with known flaws were nitrided. A seven hole pattern was sufficient to allow complete nitriding (60.7 percent weight gain) throughout the two-inch diameter hub when starting with a 1.71 g/cm^3 green density. The nitrided pieces were subjected to rapid heating to 2100°F, held 30 minutes, then cooled and showed no spalling or other failure.

Three deswirl rotors, S/Ns 191, 192, and 193 were shipped to Garrett; all had some cracks from processing. The most obviously cracked pieces were subjected to a 2100°F cycle and showed no crack growth or spalling.

Figure 67 shows the metal pattern, the organic mold and a processed casting.

3.8 Seal Rings

Several 4-inch long cylinders (approximately 8.8 inches ID and 9.3 inches OD), suitable for manufacturing seal rings at Koppers Company were prenitrided and were visually (30x) and x-ray acceptable. Three machined rings were nitrided and returned for wear test evaluation. Another ring is ready to be nitrided.

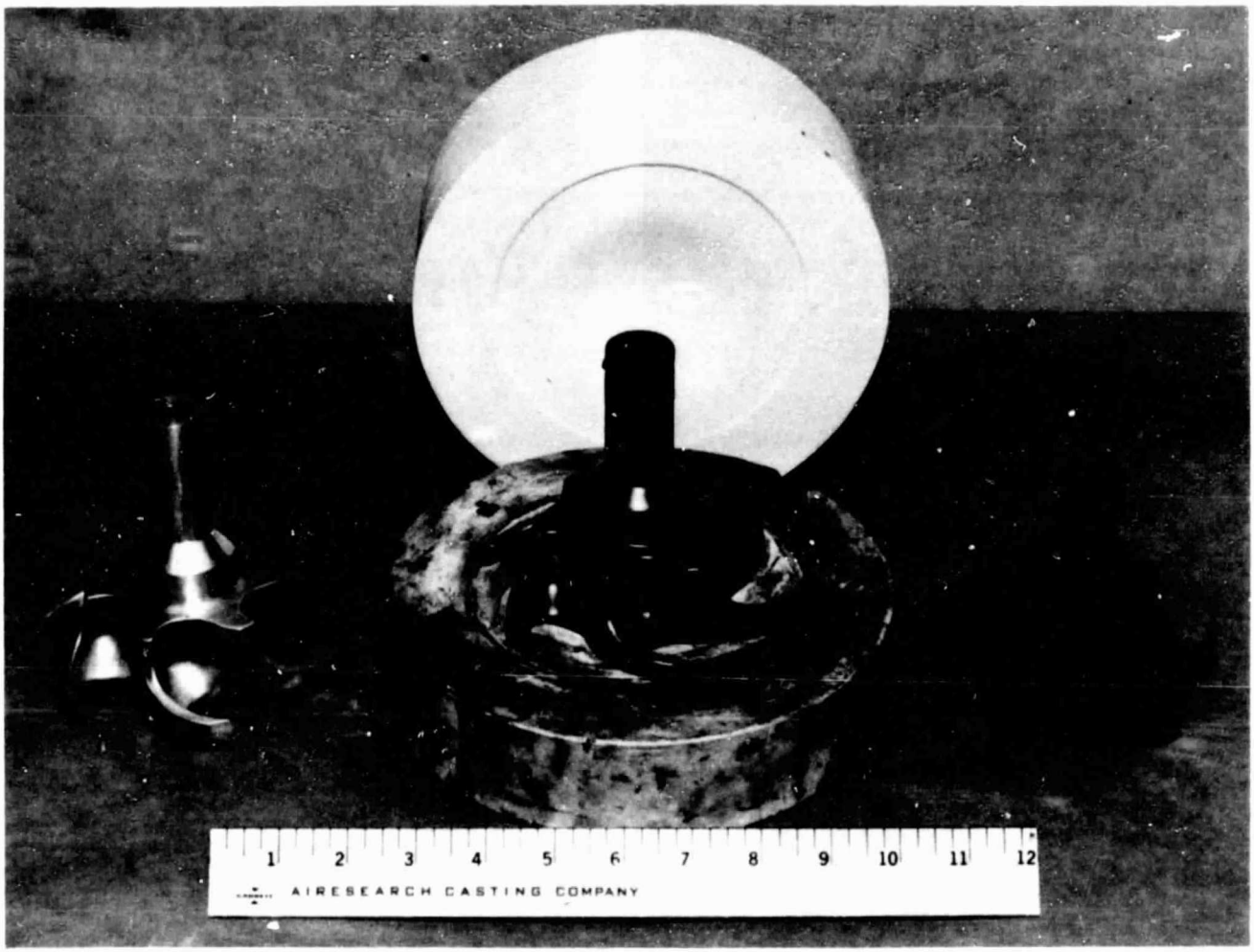

Figure 67. Deswirl Rotor Showing From Left to Right the Metal Pattern, Organic Mold on Plaster Base and Cast Part.

APPENDIX C

THE CARBORUNDUM COMPANY
(UNIQUE WORK)
ADVANCED GAS TURBINE (AGT) POWERTRAIN SYSTEM DEVELOPMENT PROGRAM
FIFTH AGT SEMIANNUAL TECHNICAL
PROGRESS REPORT

1. BACKGROUND

This report summarizes the work carried out by the Carborundum Company during the period from January 1, 1982 to June 30, 1982 for the Garrett Advanced Gas Turbine Powertrain System Development Program authorized under NASA Contract DEN3-167 and sponsored by the Department of Energy (DOE).

As a major subcontractor to the program, Carborundum is required to develop silicon carbide components for the hot flow path of the AGT engine.

Injection molding, slip casting, and green machining were the fabrication processes selected to produce hardware for the program.

Ceramic fabrication technology has been successfully demonstrated to produce complex shapes economically with precision on small items such as backshrouds, stators, vanes, duct spacers, and large components such as turbine shrouds, combustor baffles and transition ducts. At the beginning of the program, maximum cross sections for injection molded components were limited to an approximate 1-inch thickness. Technical progress now has significantly extended cross section capabilities so that large and complex components can be successfully produced to net shape with minimal grinding required. The development of two SiC materials designated Hexoloy™ KX-01 (fine grain RBSiC) and Hexoloy™ KX-02 (ultrafine grain RBSiC) represented significant strength improvements that when optimized, will apply to a variety of components.

Activities during this period addressed properties optimization of all the Hexoloy materials, and also optimization of fabrication and other processing parameters for the static structures.

2. ROTOR MATERIAL DEVELOPMENT

As reported in the last semiannual report, all effort on this phase of development activity has been suspended due to funding constraints.

3. STATIC STRUCTURES

3.1 Stator Segment

The injection molding process was selected for fabrication development of the stator assembly in Hexoloy™SA; a sintered alpha silicon carbide material. During this reporting period, the injection molding process was further refined to produce stator segments to near net shape which exhibited an absence of flaws such as blisters, sink and burn marks, and flow lines in regions that were to be left unground.

There was substantial activity on this part during the period. The highlights of this activity is as follows:

- Injection molding tool was modified to produce segments with adequate grinding stock. Parts produced using this tool were found to have sufficient stock on all surfaces to allow for grinding

- The tool also was modified to eliminate surface imperfections, detected in the trailing edge region of the segments, during NDE

- Precise fixtures for grinding and dimensional inspection of stator segments were fabricated. Inspection fixtures and verifying the OD/ID dimensions of the stator assembly were supplied by Carborundum to the grinding supplier and Garrett Quality Control

- Four complete sets of stator segments were ground and returned to Carborundum for further processing
- At Garrett request, two changes were made in the grinding/finishing of stator segments. The first of these involved increasing the total gap between segments from 0.015 to 0.020 inch nominal. This was not a print change, but a clarification of print interpretation. The second involved radiusing the intersection of the OD arc and the flat on the turbine shroud. This was done to reduce the relatively sharp edge left in this area after molding and grinding
- Two complete sets of stator segments (19 segments per set) and two spare segments (one per set) were shipped to Garrett for rig tests and possible engine qualification during the period. The other two sets are in process
- Twenty-five unground segments are being held in inventory and will be ground as necessary or at Garrett request

Approximately 250 stator segments were molded early in the reporting period. The aforementioned segments, which are in process or shipped, were generated from this molding. The process refinements instituted and processing parameters established have allowed Carborundum to develop the methodology to produce high quality stator segments which have total interchangeability.

3.2 Turbine Shroud

Since the turbine shroud has a variable wall and a complex shape with precise contours, injection molding was selected to produce the part in Hexoloy™SA. The finished part, which weighs approximately 10 pounds, represents the largest single piece component ever injection molded in this material.

All molding of these parts was accomplished using a 1000-ton reciprocating screw injection molding machine equipped with microprocessor controls. Key variables investigated in molding were material temperature, injection velocity, and cooling times.

Other activity on this component during the period was as follows:

- As discussed in the last period report, 43 shrouds were molded using a matrix of molding conditions and two different compositions to vary the shrink rate. This molding produced several parts that appeared visually good and exhibited few flow lines
- Several shrouds from this molding were baked; all the initial baked parts exhibited cracks. To minimize stress concentrations which possibly could result in cracks, a generous fillet radius was applied to the slot detail on the flange of the molded part. It is considered that this geometric change, was at least partially responsible for the production of the first crack-free shroud in March 1982
- Flatness of the flange face was a major problem with sintered shrouds; flange distortion occurred during sintering. Extensive testing showed that density differentials within the green and fired radial sections were negligible and, thus, not the probable cause of flange distortion. Several approaches were taken to solve the flange distortion problem. Among these were removing the flange sections between the mounting tabs, distorting the flange of the "as molded" part in the opposite direction of the sintering distortion, and insulating the flange during sintering. Improvement of distortion was noted during some of these tests; however, none solved the problem. Investigations are continuing to find a solution to this distortion problem
- The crack-free shroud produced in March 1982 was sent to the grinder. Fixtures and grinding methodology were developed. Grinding was commenced in June 1982 with an anticipated completion date of July 1982. Due to flange distortion it is expected that grinding will produce a part in which some minor areas are not completely cleaned up

- The injection molding tool was further modified to remove the flange slots

- Three shrouds (unground) were shipped to Garrett at their request. These shrouds were of the design that had the flange removed except for the locating tabs

- A total of fifty-three shrouds were molded during the period at the custom molder using the modified tool and two mix compositions. Several of these presently are being processed

- Special sintering fixtures are being fabricated and will be evaluated to reduce flange distortion when complete. One of these is directed towards solving the problem during sintering, and one is a post sintering procedure that involves a secondary sintering step to straighten the distorted flange

3.3 Combustor Baffle

Slip casting was selected as the fabrication method appropriate to produce the combustor baffle in Hexoloy™SA. Slip compositions have been developed that are capable of producing the 0.400-inch wall thickness required for this part. During this 6-month period, the slip casting development effort emphasized process improvements/innovations which would produce baffles that were of correct size for grinding and crack-free.

Highlights of the activity on this component during the period are as follows:

- Approximately 50 baffles were cast during the period. These were produced using varying compositions to produce the desired shrinkage and improve green strength

- New casting molds were produced to increase the fillet radius at the base of the legs (struts)

- Standard size molds produced parts that were oversize. This problem was addressed through two different development paths. One involved mix compositions that were changed to increase shrinkage during sintering. The second involved making smaller models and molds using materials with shrinkage higher than those used to make the standard models

- The higher shrinkage compositions were used to cast several parts. Though green strength was an initial problem, some of these parts have been successfully processed through all fabrication operations. One of these was fully ground and hand finished and submitted for inspection and NDE. A second component looks dimensionally correct and was submitted for pregrinding inspection and NDE

- Three baffles were cast using the smaller molds cast from downsized models. These parts are being further processed, and results will be available in the next period report

- Three baffles were delivered to Garrett

  - One baffle in which the OD radius could not be blended with the overall contour due to strut interference during grinding

  - One baffle in which the contour (as mentioned above) was not blended during grinding. This part was hand-finished to produce the desired profile

  - One baffle that exhibited linear indications on the rim after initial rough grinding. This part was not hand finished, but was shipped to Garrett for review at their request

3.4 Transition Duct

At the initiation of this program, slip casting had been selected as the fabrication method for the transition duct. However, due to the fact that the casting process produces an ID that requires green machining to produce the desired dimensions and contours, casting was abandoned in favor of total green machining to net shape. Isostatically pressed billets were used to produce the green part

from which the transition ducts were machined:

- Due to a forming problem, the practice of using a contoured isopress pin to produce the ID configuration of the duct during isopressing, was abandoned. It was replaced by a method that employs an all rubber isopressing bag to produce a straight walled green cylinder. This cylinder is fully machined on the OD, ID, and length to produce the contours and dimensions required for the duct

- All green machining was performed on CNC lathes and vertical milling machines. Programs were developed to achieve the specified OD/ID contours and other design features

- Due to fabrication problems and design considerations, the transition duct ID locating features, where the struts of the combustor baffle rest, were changed two times. The original design (Drawing 3846159) incorporating pockets for strut location, was changed to a large radius annular ring on which the baffle struts rested. The final design, which was incorporated in a majority of components, replaces the large radius ID ring with a flat annular ring that is perpendicular to the duct wall. This design is per Garrett Drawing 3846232

- Six ducts were shipped to Garrett during the period. The internal design features for the combustor baffle were of various configurations as suggested by Garrett. Five of these parts were shipped completely ground and one part was shipped unground

- The remainder of the ducts to complete the commitment to Garrett have been processed through green machining or sintering. All parts in the system have been fabricated to Garrett Drawing 3846232

3.5 Turbine Backshroud

The turbine backshroud is being developed and fabricated by green machining isostatically pressed blanks. These blanks are sintered per established procedures and dense ground to develop the final dimensions and contour. During the period, all the backshrouds requested by Garrett were shipped for evaluation and possible rig testing.

- Isopressed billets were produced and green machined into rough blanks from which the turbine backshroud will be final green machined on the CNC lathe

- Precise sintering fixtures were fabricated on the CNC lathe to eliminate distortion during sintering

- The CNC programs to green machine the front and back contours of the backshroud were completed

- Eight turbine backshrouds were green machined and sintered. Two of these were used to develop the lapping and grinding procedures to produce a precise contour within the tolerance band

- Backshroud contour lapping was unnecessary due to the fact that "as-fired" contours were very close to the desired tolerance band

- Six turbine backshrouds were finish ground, inspected, and put through NDE. All six shrouds were shipped to Garrett in June 1982 for evaluation and possible rig testing

Garrett has not requested any more of these components, and this item is considered complete.

4.0 COMPONENT PHOTOGRAPHS

Figures 68 through 73 contain photographs of the various components fabricated during this period. Included are photographs of the assemblies of separate components showing sequentially how the parts fit together. No backshroud photographs are included because all these components were shipped to Garrett.

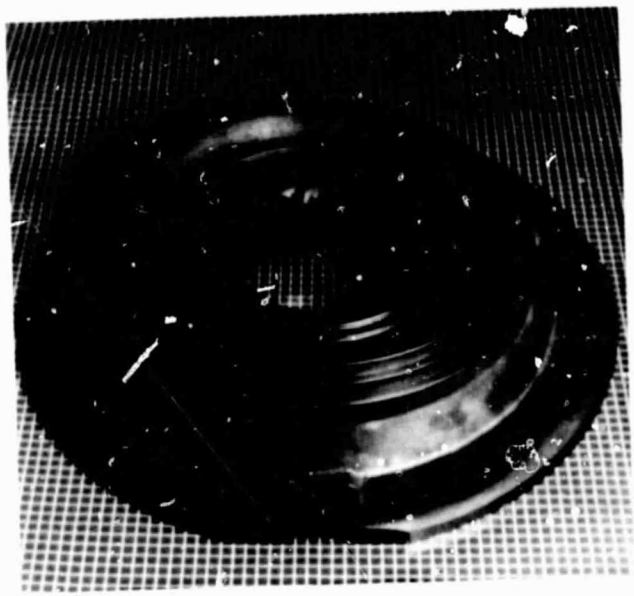

Figure 68. Turbine Shroud (Finish Ground).

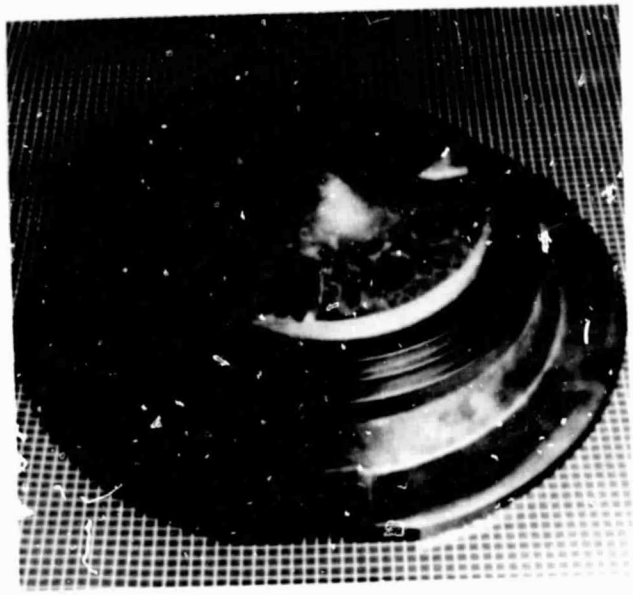

Figure 70. Combustor Baffle/Stator Segments/Turbine Shroud Assembly.

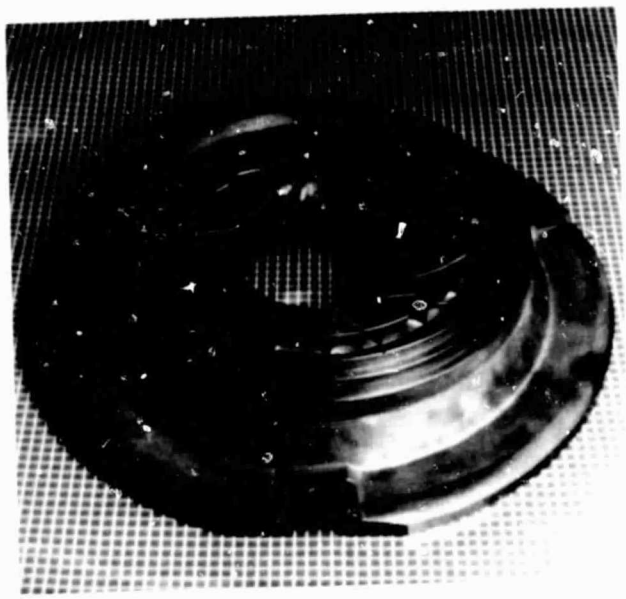

Figure 69. Stator Segments/Turbine Shroud Assembly.

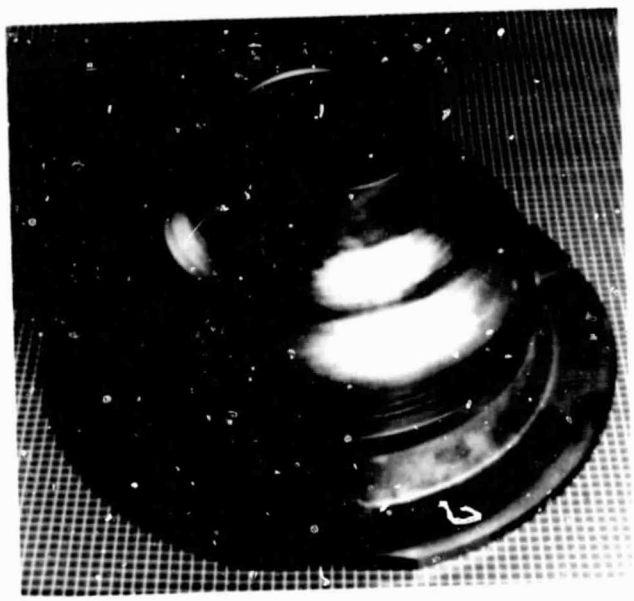

Figure 71. Transition Duct/Combustor Baffle/Stator Segments/ Turbine Shroud Assembly.

Figure 72. Turbine Shroud, Transition Duct, Combustor Baffle, and Stator Segments.

Figure 73. Turbine Shroud, Transition Duct, Combustor Baffle, Stator Segments, and Combustor Liner (Liner is Fabricated from Hexoloy™ SA).

APPENDIX D

LIST OF SYMBOLS, ABBREVIATIONS AND ACRONYMS

Acronyms	Definition
ACC	AiResearch Casting Company
AGT	advanced gas turbine
AGT101	the AGT model being developed by Garrett/Ford
Al_2O_3	aluminum oxide
AS	aluminum silicate
BN	Borazon
°C	degrees Celsius
CBO	The Carborundum Company
C_L	clearance probes
CFDC	Combined Federal Driving Cycle
CNC	computer numerical control
CO	carbon monoxide
CO_2	carbon dioxide
DAW	dual alloy wheel
DFC	diffusion flame combustor
DOE	U.S. Department of Energy
DS	directionally solidifed
ECU	electronic control unit
EDX	energy dispersive X-ray
EPA	Environmental Protection Agency
°F	degrees Fahrenheit
Ford 707	an industrial gas turbine engine by Ford
FY	fiscal year

LIST OF SYMBOLS, ABBREVIATIONS AND ACRONYMS (Contd)

Acronyms	Definition
GE	General Electric Company
HC	hydrocarbon
HCl	hydrogen chloride
Hexoloy™ KX01	Carborundum material, SiC
Hexoloy™ KX02	Carborundum material, SiC
Hexoloy™ SA	Carborundum material, SiC
Hf	halfnium
HIP	hot isostatic pressing
HP	high pressure regenerator inlet (cold side)
Hz	Hertz (frequency)
ID	inner diameter
IGV	inlet guide vane (compressor)
IR&D	internal research and development
I-112	regenerator seal coating material
JP-4	jet propulsion fuel Number 4
ksi	thousand pounds per square inch
lb/min	pounds per minute airflow
LBO	lean blowout
LCF	low cycle fatigue
LDV	laser Doppler velocimeter
LP	low pressure regenerator inlet (hot side)
"m"	Weibull modulus
MAS	magnesium aluminum silicate
MEK	methyl ethyl ketone

LIST OF SYMBOLS, ABBREVIATIONS AND ACRONYMS (Contd)

Acronyms	Definition
MENTOR II	Ford regenerator computer program
METCO 443	flame spray coating
METCO 447	flame spray coating
MgO	magnesium oxide
Mod I	first development engine
Mod II	second generation ceramic engine
MOR	modulus of rupture
N	population, number of samples
NASA	National Aeronautics and Space Administration
NGK	NGK-Locke, Inc.
NiCr	nickel chrome
NO_x	oxides of nitrogen
OD	outer diameter
PM	powder metal
P/N	part number
P_S	static pressure
psia	pounds pressure per square inch, absolute
psid	pounds pressure per square inch, differential
psig	pounds pressure per square inch, gauge
P_T	total pressure
PWM	pulse width modulated
RBN 104	ACC RBSN material
RBN 124	ACC RBSN material
RBSiC	reaction bonded silicon carbide

LIST OF SYMBOLS, ABBREVIATIONS AND ACRONYMS (Contd)

Acronyms	Definition
RBSN	reaction bonded silicon nitride
RM-1	Ford rotor material, first generation
RM-2	Ford rotor material, second generation
RMS	root mean square
RPD	reference powertrain design
rpm	revolutions per minute
RSSiC	reaction sintered silicon carbide
SEM	scanning electron microscopy
SiC	silicon carbide
Si_3N_4	silicon nitride
SMD	sauter mean diameter
S/N	serial number
SNN 522	ACC sintered silicon nitride
SN-50	NGK silicon nitride material
S/R	stress rupture
SRBSN	sintered RBSN
TC	thermocouple
TD	theoretical density
TIR	total indicator reading
TIT	turbine inlet temperature
TRW	Thompson Ramo Woldridge, Inc.
T_T	total temperature
T-T	total-to-total
VIGV	variable inlet guide vane

LIST OF SYMBOLS, ABBREVIATIONS AND ACRONYMS (Contd)

Acronyms	Definition
W	tungsten
W-K	Wayne-Kerr
yo-yo	Astroloy heat treat cycle
Y_2O_3	yttrium oxide
α-SiC	Carborundum material, Hexoloy™
β	beta
θ	temperature/temperature standard
$\mu\epsilon$	micro strain
σ	pressure/pressure standard
σ_A	characteristic strength

REFERENCES

1. Garrett Turbine Engine Company, "Advanced Gas Turbine (AGT) Powertrain System Development for Automotive Applications", Semiannual Progress Report Number 1 (October 1979 through June 1980), Report No. NASA CR-165175, November 1980, Contract No. DEN3-167.

2. Garrett Turbine Engine Company, "Advanced Gas Turbine (AGT) Powertrain System Development for Automotive Applications", Semiannual Progress Report Number 2. (July 1980 through December 1980), Report No. NASA CR-165329, June 1981, Contract No. DEN3-167.

3. Garrett Turbine Engine Company, "Advanced Gas Turbine (AGT) Powertrain System Development for Automotive Applications", Semiannual Progress Report Number 3 (January 1981 through June 1981), Report No. NASA CR-167901, December 1981, Contract No. DEN3-167.

4. Garrett Turbine Engine Company, "Advanced Gas Turbine (AGT) Powertrain System Development for Automotive Applications", Semiannual Progress Report Number 4. (July 1981 through December 1981), Report No. NASA CP-167983, June 1982, Contract No. DEN3-167.

5. D.N. Anderson, "Ultra-Lean Combustion at High Inlet Temperatures", Report No. NASA TM-81640, Prepared for Twenty-Sixth Annual International Gas Turbine Conference (March 8-12, 1981), Interagency Agreement EC-77-A-31-1011.